R. & M. No. 2881
(13,465, 13,718)
A.R.C. Technical Report

MINISTRY OF SUPPLY

AERONAUTICAL RESEARCH COUNCIL
REPORTS AND MEMORANDA

Control Testing in Wind Tunnels

By

L. W. BRYANT, B.Sc., A.R.C.S., and H. C. GARNER, B.A.
of the Aerodynamics Division, N.P.L.

LONDON: HER MAJESTY'S STATIONERY OFFICE
1956
FIFTEEN SHILLINGS NET

Control Testing in Wind Tunnels

By

L. W. BRYANT, B.Sc., A.R.C.S., and H. C. GARNER, B.A.

of the Aerodynamics Division, N.P.L.

Reports and Memoranda No. 2881*

January, 1951

Summary.—If *ad hoc* wind-tunnel work on controls is to be of value it is essential that the same precautions should be taken as are necessary for fundamental research. For the model there must be careful selection of material and accurate finish. Attention must be paid during the experiments to the observation and control of transition in the boundary layer; a suitable technique for doing this is outlined.

Control power may be measured on complete models of reasonable size, but usually hinge moments can only be measured satisfactorily on partial models, which provide control surfaces large enough for accurate reproduction of contours and detailed features. The great care and time involved in the construction of models and testing of controls for design purposes are frequently not justified when the only purpose is to determine the effects of balance, gaps, or small changes of shape. On the model scale the main object of tests should be to determine the properties of the basic control shape chosen by the designer, recognising that there will in general be differences of detail in the actual aircraft for which a margin must be allowed.

Some notes are included on the correction of tunnel measurements for Reynolds number. It is suggested that the basis of this correction should be the slope of the lift curve against incidence for the aerofoil section or sections used. For a given Reynolds number and position of boundary-layer transition the lift slope is related to its value in potential flow by a ratio which can be estimated from generalised charts. On this basis the prediction of Reynolds number effect on control characteristics should be satisfactory when the full-scale boundary-layer conditions can be specified. Though more evidence is required for swept wings and high-speed flow, a procedure to deal with sweepback and compressibility is included.

The models suitable for control testing are invariably large for the size of tunnel available for the tests, and the estimate of tunnel interference corrections becomes a major consideration. The use of open-jet tunnels for such experiments is not recommended. Tests of partial models are best carried out in closed tunnels of rectangular or octagonal section. It is essential that a systematic scheme of calculation should be undertaken by wind-tunnel staff for each tunnel likely to be used for the testing of large models. Certain tables of numerical values can be drawn up so that tunnel operators can do their own computing of the tunnel corrections; instructions for this are given in Appendix II. Corrections are required for blockage and for tunnel-wall constraint on the flow associated with the lift on the model. The procedures to be followed in computing corrections for two-dimensional and three-dimensional experiments are described in detail.

The numerical significance of the corrections for wind-tunnel interference and for scale effect is discussed at the end of the report with illustrations from worked examples. In the case of control derivatives it is clear that corrections for scale effect are often the more important and should be estimated as part of the routine.

* This report comprises A.R.C. 13,465, A.R.C. 13,718, and the Appendix to A.R.C. 10,936, which forms the present Appendix II.

Published with the permission of the Director, National Physical Laboratory.

CONTENTS

1. *Introduction.*—Experience has shown very clearly that, unless considerable care is taken both with the construction of the model and with the conditions of test, control testing in a wind tunnel has little value. The interpretation of the results is in any case not an easy matter. The basis of design of controls must always be a carefully organised research in wind tunnels combined with co-ordinated measurements on the full scale ; and to be of value *ad hoc* testing must adhere in the main to the same rules of procedure as have been found essential in fundamental research. If this is not practicable it is far better to rely on estimates from standard formulae and collected data.

Systematic research on controls has so far been confined in the main to the study of the effects of the boundary layers on the properties of control flaps. One of the objects of this study is to establish a firm basis for the extrapolation of model results to the full-scale Reynolds number in the absence of shock-waves. It has been found that the three-dimensional characteristics of unswept wings can be related to those in two-dimensional flow. The properties of a given aerofoil section can be related closely to the slope of the lift-incidence curve expressed as a fraction of the corresponding value in potential flow. This ratio can be estimated from generalised charts, together with its variation from model to full-scale Reynolds number; it can then be used for the interpretation of the measured quantities from the model tests. The process is not yet fully developed for swept wings, but suggestions are put forward in this report for a procedure to be adopted until further investigation reveals any essential changes in principle. The behaviour of the aerofoil section and especially of control flaps is sensitive in general to the position of the transition, where the boundary layer changes from laminar to turbulent flow; it is therefore important to observe the transition in the model experiments and in addition to find the effect of artificially changing its position. This information can be used to assess the likely uncertainties in the prediction of the effects of Reynolds number, and in favourable cases to improve the accuracy of this prediction.

If the model is of a complete aircraft to a comparatively small scale, moments on the aircraft due to control deflections may be determined with reasonable confidence, but in general hinge moments can only be measured satisfactorily on partial models made to a larger scale than is possible with complete models. This is necessary in order to reproduce with sufficient precision the contours of the control surface, the hinge location, and the finish of nose and trailing edges, all of which will materially affect hinge moments. It is considered that, until more is known of modern swept wings, control testing on models should primarily be concerned with smooth surfaces and sealed gaps, with complications of balance and gaps as far as possible treated as a separate problem. There is then a reasonable prospect of extrapolating to full-scale Reynolds number. Isolated tests which do not include a test of the smooth plain control, unbalanced, may well prove to be misleading; several changes in the parameters must be tested and compared. At higher incidences in particular the effect of gaps may be serious, and the scale effect on them unpredictable. Without them and other complicating details the procedure outlined in this report is applicable, as far as present knowledge goes, to all tests up to the approach of the stall. The stall of the sections in two-dimensional flow may give some indication of the incidence or lift coefficient at which the tip stall of a swept wing should occur on the model and on full-scale. Unfortunately there has been so far a large discrepancy between the two in most cases, and it is obvious that short of some device for postponing the tip stall of the model, only a higher Reynolds number of test can give reliable information concerning controls at the lowest speeds of flight.

2. *Construction of the Model.*—It is important that the fixed surfaces of wings and tail organs should be finished as smoothly and accurately as possible ; smoothness is particularly necessary to ensure maximum accuracy of measurement, because it is essential that transition in the boundary layer should not be precipitated by local imperfections of the surface. The flaps must be made with special care as true as possible to contours, particular attention being paid to the finish at the trailing edge, to the accuracy of construction at the nose of the control and to the fitting of the flap into its shroud by the location of the hinges.

Models for use in the majority of existing tunnels will be made of wood. It is desirable that they should be built up in laminated well-seasoned mahogany or other suitable hard wood,

except for separate surfaces small in area, which may sometimes be made out of the solid. Soft woods are not suitable unless the model is required only for a short test immediately after the completion. A reliable filler should be used on the woodwork before applying polish or varnish. The harder, more durable finishes now favoured in some laboratories have been found at times to reduce the accuracy attainable where curvature is great, unless an inordinate amount of time is spent in rubbing down. A well-polished varnish finish is often to be preferred for ordinary work in atmospheric tunnels as it saves time in manufacture. The harder finish is of course essential if active chemicals or the ' china-clay technique ' for observing transition are likely to be used, or if the model is to be subjected to high-pressure air.

It has been found necessary to use a close-grained wood-like box, or one of the proprietary plastic materials of fine texture free from layers to construct the trailing-edge portion of a flap, or for the whole flap if it is a small one. The important point here is to reproduce the equivalent trailing-edge angle accurately. It is useful to groove the trailing edge (if of wood) into the body of a control flap so that movement is possible without distortion under temperature and moisture changes.

The span of a model should not exceed $0{\cdot}7$ of the breadth of the tunnel (or the height if the model is vertical) and the ratio of chord to tunnel height (or breadth for a vertical model) should not be greater than $0{\cdot}5$ over any part of the span; further, the ratio of mean chord to tunnel height (or breadth) should not exceed $0{\cdot}35$. The mean chord should be at least 5 in. in order that the required accuracy of manufacture may be possible. Ailerons may be tested on part wings of half or nearly half the total wing span. Tail organs may be tested with a stub body.

It is preferable to seal the gap at the nose, otherwise the greatest care should be taken that the gap is known accurately along the whole length of the flap. When the gap on the actual aircraft is known it is often better to correct for it, using a sealed-nose model test as basis; correction data exist for this purpose. Hinges should be well cleaned and lubricated ball-bearings held in brackets rigidly attached to the shroud; crossed springs are sometimes advisable. Gaps around hinge brackets must be kept to a minimum.

The need for accuracy in the construction of flaps may be illustrated by some figures from National Physical Laboratory tests:

One degree increase of trailing-edge angle gives $\Delta b_2 = +0{\cdot}04$.

$0{\cdot}01$ increase of centre-line camber of the control gives $\Delta C_H = -0{\cdot}03$.

The procedure for tailplane and elevator testing when determining the stick-free stability of new aircraft, as laid down by Wright Field and the U.S. Bureau of Aeronautics, is to use an actual tail unit or half unit or a large-scale model of the actual unit in a high-speed tunnel. It is argued that the ideally finished model is certain to yield erroneous results, especially if the trailing edge is ' razor sharp '. High speed is desirable to show up any effects of elastic distortion. Any necessary adjustments of balance are made forward of the hinge-line and not by tampering with elevator contour or trailing-edge angle.

These recommendations can only be adopted when a large and high-speed tunnel is available; even then they can be satisfactory only when several production specimens are tested, in view of the usually unavoidable variations in manufacture. In this country when a comparatively low Reynolds number of test must be accepted it would appear to be preferable to use a carefully made solid model, recognising that what is being tested is the basic geometrical design, and that due allowance must be made in interpreting the results for any likely effects of elastic distortion or errors in manufacture.

3. *Observation and Control of Transition in the Boundary Layer.*—In order to make it possible to interpret the results of model tests on control characteristics it is necessary to adopt a procedure which gives sufficient information about the effects of boundary-layer transition. Bryant and Batson[23] (1944) have suggested the following tests as in general providing the requisite data.

The model is tested first over the required range of incidence and control angle with wings smooth, *i.e.*, without wires to locate transition. Then over the range of incidence within 5-deg of minimum drag with flap angles between $\pm$ 10-deg the tests are repeated, (*a*) with a wire at 0·1 chord from the leading edge on both upper and lower surfaces, (*b*) with a wire at 0·1 chord on the upper surface only. In addition the positions of natural transition on both upper and lower surfaces must be observed for the same ranges of values of incidence and flap angle as for the (*a*) and (*b*) tests. This can be done by evaporation tests as described in Refs. 20, 21, and 22. Laminar separation, if it occurs, must be suppressed by placing a wire about 0·1 chord in front of the position of separation. This is best determined by coating a portion of the wing near the observed transition region with lead acetate and exploring close to the surface with a fine tube from which H_2S is slowly emerging. Any backward flow in the boundary layer will be indicated by the stain, and the actual position of any separation can easily be located as the position when flow at the surface is neither backward nor forward. The beginning of turbulent separation at the trailing edge may be explored in a similar manner, and the incidence or flap angle at which this occurs may be determined; these observations are of value if the curves of control coefficients are notably non-linear.

The tests with wires on both surfaces at the same distance from the leading edge are intended to cover the case where transition occurs on the full scale in front of the minimum pressure point at the optimum C_L owing to surface imperfections, whilst the tests with one wire only cover the effects of forward movement of transition on the upper surface on the full scale due to change of incidence or to change of flap angle.

3.1. *Size of Transition Wires.*—It has been the custom to determine the wire diameter to fix transition from the relation $Vd/\nu > 600$, where V is the wind speed in the tunnel, d the wire diameter and ν the kinematic viscosity of the air. The conditions of the boundary layers at the trailing edge, so far as they affect control forces, are not specially sensitive to wire diameter, provided it is large enough to cause transition to take place at the wire without a subsequent return to a laminar layer further downstream. The criterion $Vd/\nu > 600$ is a rough interpretation of the more exact criterion $ud/\nu > 400$, given by Fage[24] (1943), where u is the velocity in the boundary layer at the position at the highest point of the wire surface when the wire is absent. But the criterion should vary with the Reynolds number of test and with the distance of the wire from the leading edge. Fig. 1, based on flat-plate theory, may be used for determining wire size on low-drag types of section. If x is the distance of the wire from the leading edge, the thickness, δ, of the boundary layer is of the order given by

$$V\delta/\nu = 5{\cdot}84\sqrt{(Vx/\nu)} .$$

From the graph of Fig. 1 the minimum value of Vd/ν to ensure final transition can be read off when the value of Vx/ν is known. The graph is determined from the basis $ud/\nu = 400$. It is advisable to choose d so that Vd/ν is at least some 20 per cent greater than the value read off the graph.

4. *Corrections for Tunnel-Wall Interference.*—Where hinge moments and the effects of small modifications to a control are to be investigated the use of part models is almost unavoidable. The part models are invariably large for the size of tunnel available for the tests, and the estimate of tunnel interference corrections becomes a major consideration. In general it would seem to be essential that a systematic scheme of calculation should be undertaken by a wind-tunnel staff for each tunnel likely to be used for the testing of large models. Certain tables of numerical values can be drawn up so that tunnel operators can do their own computing of tunnel corrections. The tables should give the upwash at a fair number of selected points in the working-section of the tunnel due to images of simple horse-shoe vortices of varying span situated in the region where a wing under test is likely to be placed. The procedure for doing this is described in Appendix II.

The first correction to be applied is the so-called ' blockage ' correction, which is represented by an increment to the speed of test. The main correction is for the constraint of the tunnel

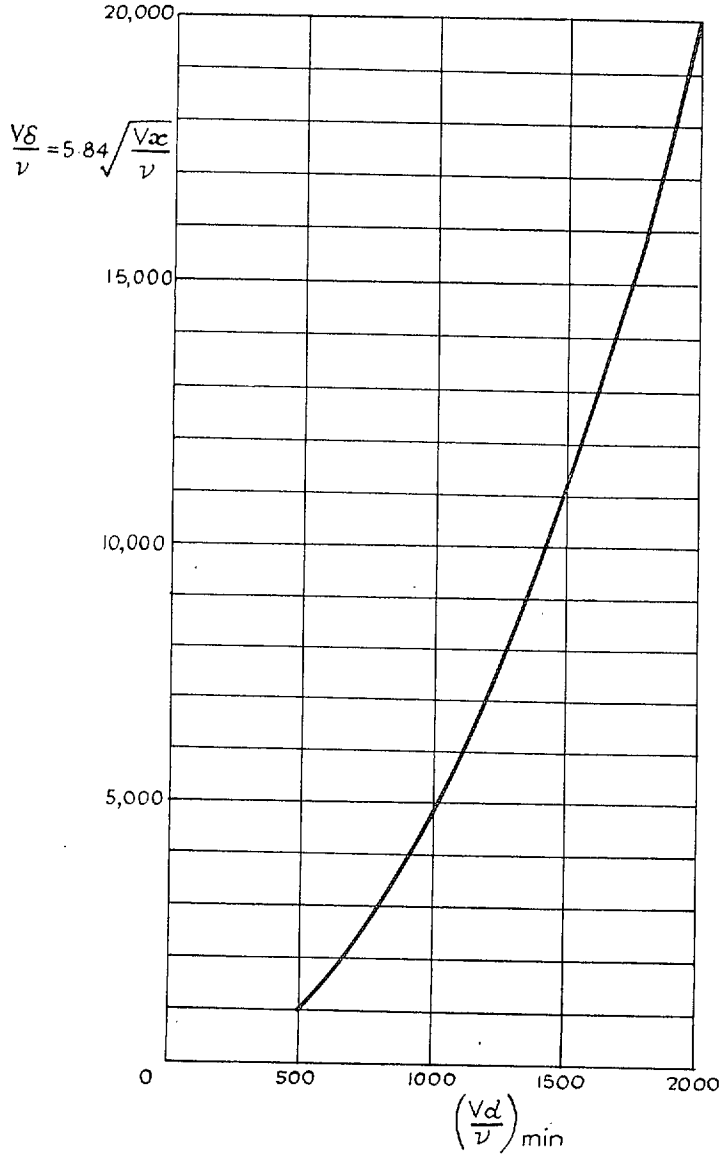

FIG. 1. Graph to determine the size of transition wire.

walls on the flow due to the vorticity on the surface of the wing and in the wake; this is equivalent to a distribution of upwash induced in the neighbourhood of the model, and may be represented roughly by a correction to incidence and a residual local incidence and superposed curvature of flow at each section of the model. The residual interference is interpreted as corrections to the aerodynamic forces and moments.

A really satisfactory computation of tunnel-wall corrections is best made by first estimating the lift distribution for the model in a free stream using lifting-line theory, then employing the tables to compute downwash distributions at the model in the tunnel due to the images arising from this assumed lift distribution associated with the measured lift and pitching moment. For fundamental research work this procedure has been used at the N.P.L. when the model is large. But if control testing becomes a considerable part of wind-tunnel programmes time and labour can be saved by adopting approximate interference corrections based on calculations for elliptically loaded wings (section 4.4) or a simple combination of part-span uniform loadings to cover the case of flaps and ailerons (section 4.5).

4.1. *Blockage Correction.*—The space occupied by the model and its wake in a closed tunnel effectively reduces the tunnel cross-section and causes an increase of longitudinal velocity which does not exist in a free stream. It is shown by Young[1] (1945) that at low speeds the solid blockage correction due to a two-dimensional model itself may usually* be estimated with sufficient accuracy by the formula

$$\frac{(\delta V)}{V} = 0{\cdot}62\frac{A'}{h^2},$$

where A' is the area of the wing section

(δV) is the increment to the speed of test, V

h is the dimension of the tunnel at right-angles to the span of the model.

The wake blockage correction should be related to the drag coefficient of the wing

$$C_D = \frac{\text{profile drag force per unit span}}{\frac{1}{2}\rho V^2 c} = \frac{\text{profile drag force}}{\frac{1}{2}\rho V^2 S},$$

when this can be measured or estimated†. The formula

$$\frac{(\delta V)}{V} = \frac{C_D S}{4C},$$

where S is the surface area of the wing

C is the cross-sectional area of the tunnel

has been suggested by Thompson[3] (1947) and is recommended for general use at low speeds.

Thus in incompressible two-dimensional flow the overall blockage correction is

$$\frac{(\Delta V)}{V} = 0{\cdot}62\frac{A'}{h^2} + \frac{C_D}{4}\cdot\frac{c}{h}. \qquad \ldots\ \ldots\ \ldots\ \ldots\ \ldots \quad (1)$$

This formula can easily be extended to cases of three-dimensional wings for which

$$\frac{(\Delta V)}{V} = 0{\cdot}62\frac{V'}{Ch} + \frac{C_D}{4}\frac{S}{C}, \qquad \ldots\ \ldots\ \ldots\ \ldots\ \ldots \quad (2)$$

where V' is the volume of the model.

For a complete aircraft model the blockage effect of the wake of the fuselage may be neglected, and following Ref. 1 the formula

$$\frac{(\Delta V)}{V} = 0{\cdot}65\frac{V'}{Ch} + \frac{C_D S}{4C} \qquad \ldots\ \ldots\ \ldots\ \ldots\ \ldots\ \ldots \quad (3)$$

is estimated to be accurate within $\pm$ 10 per cent.

---

* Young has only considered sections of thickness/chord ratio $t/c = 0{\cdot}1$ and $0{\cdot}2$. For conventional aerofoil shapes, Thompson[3] recommends the approximate formula for solid blockage

$$\frac{(\delta V)}{V} = \frac{\pi}{6}\left(1 + 1{\cdot}2\frac{t}{c}\right)\frac{A'}{h^2}.$$

† When C_D cannot be measured or estimated, the wake blockage correction may be applied in Glauert's[2] form (1933)

$$\frac{(\delta V)}{V} = \frac{\eta t}{h}, \text{ where, approximately, } \eta = 0{\cdot}50\frac{t}{c}.$$

But it is emphasised that in the case of a low-drag wing this formula will seriously overestimate the wake blockage.

The factors for compressibility are considered by Thompson (Ref. 3, p. 17), who recommends

$$\frac{1}{\beta^3} \text{ for solid blockage;}$$

$$\frac{1}{\beta^2} \text{ for wake blockage*;}$$

where $$\beta = \sqrt{(1 - M^2)},$$

in two and three dimensions and for bodies of revolution.

Thus from equations (1), (2) and (3) the blockage in a closed rectangular subsonic high-speed tunnel is given by the formulae:

for a two-dimensional wing,

$$\frac{(\Delta V)}{V} = \frac{0{\cdot}62}{\beta^3}\frac{A'}{h^2} + \frac{C_D}{4\beta^2}\frac{c}{h}$$

for a three-dimensional wing,

$$\frac{(\Delta V)}{V} = \frac{0{\cdot}62}{\beta^3}\frac{V'}{Ch} + \frac{C_D}{4\beta^2}\frac{S}{C} \qquad \ldots \quad (4)$$

for a complete aircraft model,

$$\frac{(\Delta V)}{V} = \frac{0{\cdot}65}{\beta^3}\frac{V'}{Ch} + \frac{C_D}{4\beta^2}\frac{S}{C}$$

The blockage correction with a given model in a tunnel of the open-jet type is of the opposite sign and of half the magnitude of the correction in a closed tunnel of the same dimensions (Ref. 2, p. 53).

4.2. *Two-dimensional Interference Correction.*—The main wall interference arises from the circulation round the wing. The image system of vortices, required to satisfy the boundary conditions at the tunnel wall, produces a distribution of velocity normal to the plan-form. For a two-dimensional wing spanning a closed rectangular tunnel of height h, this upwash is normally expanded in even powers of c/h. For $c/h < 1/3$, it is only necessary to consider the first term and the interference in incompressible potential flow is equivalent to an increase in incidence

$$(\Delta\alpha) = \frac{\pi}{96}\left(\frac{c}{h}\right)^2 (C_L' + 4C_m'), \qquad \ldots \quad (5)$$

where C_L' is the measured lift coefficient and C_m' the measured pitching-moment coefficient with respect to the quarter-chord point, together with a change of camber $(\Delta\gamma)$ given by

$$2(\Delta\gamma) = \frac{\pi}{96}\left(\frac{c}{h}\right)^2 C_L', \qquad \ldots \quad (6)$$

defined by a parabolic arc of maximum height $(\Delta\gamma) \cdot c$ above its chord at the centre [Ref. 4, Miss Lyon (1942)].

The expression for $(\Delta\alpha)$ in (5) may also be written in the form

$$(\Delta\alpha) = \frac{\pi}{48}\left(\frac{c}{h}\right)^2 C_L'(1 - 2l), \qquad \ldots \quad (7)$$

where lc is the distance of the centre of pressure behind the leading edge. On the basis of the

* When extensive shock-waves are present, these theoretical corrections are too small and it seems best to use the factor $1/\beta^3$ throughout (Ref. 3, p. 5).

two-dimensional potential flow past a thin plate due to a pure incidence change

$$l = l_1 = \tfrac{1}{4}$$

and due to a deflected flap

$$l = l_2 = \frac{2(\pi - \theta_1) + 4\sin\theta_1 - \sin 2\theta_1}{8(\pi - \theta_1 + \sin\theta_1)} \Bigg\} \quad \ldots \quad (8)$$

where

$$E = \frac{\text{flap chord}}{\text{wing chord}} = \frac{c_f}{c} = \frac{1 + \cos\theta_1}{2}.$$

Values of l_2 from (8) are given in Table 1. Experimental values (Refs. 11 and 15) of l_2 are found to be about 7 per cent greater.

TABLE 1

Theoretical Values of l_2 for a Thin Plate

E*	0·08	0·10	0·15	0·20	0·25	0·30	0·35	0·40	0·45	0·50
l_2	0·474	0·467	0·451	0·435	0·420	0·405	0·390	0·375	0·361	0·347

In general the measured lift coefficient C_L' is the sum of $(C_L)_1$ due to pure incidence and $(C_L)_2$ due to flap deflection, and it follows from (6) and (7) that

$$\left.\begin{aligned} (\Delta\alpha) &= \frac{\pi}{48}\left(\frac{c}{h}\right)^2 \{(C_L)_1(1 - 2l_1) + (C_L)_2(1 - 2l_2)\} \\ 2(\Delta\gamma) &= \frac{\pi}{96}\left(\frac{c}{h}\right)^2 \{(C_L)_1 + (C_L)_2\} \end{aligned}\right\} \quad \ldots \quad (9)$$

For some purposes when the stalling condition is not too nearly approached it is usual to correct the measured incidence by the quantity (in radians)

$$\{(\Delta\alpha) + 2(\Delta\gamma)\} = \frac{\pi}{96}\left(\frac{c}{h}\right)^2 \{(C_L)_1(3 - 4l_1) + (C_L)_2(3 - 4l_2)\}. \quad \ldots \quad (10)$$

But evidence given later in this section [*see* (14)] suggests that the ratio

$$\frac{\partial C_L}{\partial\gamma} \Big/ \frac{\partial C_L}{\partial\alpha} < 2,$$

and it is preferable to correct the incidence according to the relation (9) and also to correct the measured lift coefficient C_L' by

$$(\Delta C_L) = -\frac{\pi}{192} \cdot \left(\frac{c}{h}\right)^2 \cdot C_L' \cdot \frac{\partial C_L}{\partial\gamma}. \quad \ldots \quad (11)$$

Similarly, when pitching and hinge moments are being determined, the same correction is applied to α, and the measured values C_m' and C_H' are corrected by the respective amounts

$$\left.\begin{aligned} (\Delta C_m) &= -\frac{\pi}{192}\left(\frac{c}{h}\right)^2 \cdot C_L' \cdot \frac{\partial C_m}{\partial\gamma} \\ (\Delta C_H) &= -\frac{\pi}{192}\left(\frac{c}{h}\right)^2 \cdot C_L' \cdot \frac{\partial C_H}{\partial\gamma} \end{aligned}\right\} \quad \ldots \quad (11)'$$

The camber derivatives $\partial C_L/\partial\gamma$, $\partial C_m/\partial\gamma$ and $\partial C_H/\partial\gamma$ will be denoted by a', m' and b' respectively.

* For balanced controls E should be replaced by $(\lambda + 1)E$ as defined in (13).

According to the theory of potential flow past a thin plate*

$$\left.\begin{aligned}(a')_T &= \left(\frac{\partial C_L}{\partial \gamma}\right)_T = 4\pi \\ (m')_T &= \left(\frac{\partial C_m}{\partial \gamma}\right)_T = -\pi\end{aligned}\right| \quad \ldots \quad (12)$$

If the flap has nose balance, it may be verified from Ref. 16 (Thomas and Lofts, 1945) that

$$E^2(b')_T = E^2\left(\frac{\partial C_H}{\partial \gamma}\right)_T = -2(\pi - \theta_2)\cos\theta_1 - \sin 2\theta_2 \cos\theta_1 - \tfrac{4}{3}\sin^3\theta_2\,, \quad (13)'$$

where $\cos\theta_1 = 2E - 1$, $\cos\theta_2 = 2(\lambda + 1)E - 1$, λ being the chord of the nose balance as a fraction of the chord of the flap.

Without nose balance, $\theta_1 = \theta_2$ and (13)′ yields

$$E^2(b')_T = -2(\pi - \theta_1)\cos\theta_1 - \tfrac{3}{2}\sin\theta_1 - \tfrac{1}{6}\sin 3\theta_1\,. \quad \ldots \quad (13)$$

Experimentally the values of a', m', b' differ considerably from their theoretical values on account of boundary layers on the wing surface. From N.A.C.A. tests[6] (1933) on a series of aerofoil sections of varying thickness and camber at Reynolds numbers of approximately $R = 3{\cdot}2 \times 10^6$, experimental values of a' and m' have been deduced by considering those sections with parabolic camber-lines. The tests were carried out on models of rectangular plan-form of aspect ratio 6. In Ref. 6, the curves of C_L were presented uncorrected for aspect ratio and the values below have been corrected by a factor 1·405. The presented curves of C_m were already corrected to infinite aspect ratio according to lifting-line theory by a factor 1·365 and the values below have therefore been corrected by a further factor 1·03. An analysis of the relevant tests suggests roughly, that

$$a' = 4\pi - 19\frac{t}{c} - 10\alpha\,, \ (\alpha \text{ in radians})$$

$$m' = -\left(\pi - 5\frac{t}{c}\right) \text{ where } \alpha \text{ is small}$$

$$= -0{\cdot}7\pi \text{ for all values of } \frac{t}{c} \text{ near the stall } (\alpha \doteq 0{\cdot}25)\,.$$

This does not imply that thickness/chord ratio t/c has any appreciable direct influence on a' or m'. At small incidences they are approximately related to the lift slope, $\partial C_L/\partial\alpha = a_1$; for the N.A.C.A. results, corrected to infinite aspect ratio, are represented roughly by

$$a_1 = 2\pi - 3{\cdot}5\frac{t}{c}\,,$$

while theoretically (Ref. 11)

$$(a_1)_T = 2\pi\left(1 + 0{\cdot}8\frac{t}{c}\right)\,.$$

Approximately therefore

$$\frac{a_1}{(a_1)_T} = 1 - 1{\cdot}2_5\frac{t}{c}\,.$$

* There is an effect of thickness on camber derivatives (Ref. 5, section 3). For the purposes of the present report the suffix T, as applied to camber derivatives, will denote theoretical values neglecting wing thickness.

When α is small, the ratios of the camber derivatives to the theoretical values in (12) are

$$\frac{a'}{4\pi} = 1 - 1{\cdot}5\frac{t}{c};$$

$$\frac{m'}{-\pi} = 1 - 1{\cdot}6\frac{t}{c}.$$

Thus, with a probable accuracy of the order 5 per cent

$$\frac{a'}{4\pi} = \frac{m'}{-\pi} = \frac{a_1}{(a_1)_T}. \qquad \ldots\ldots\ldots\ldots\ldots\ldots\ldots \quad (14)$$

There is an indication that both a' and m' diminish numerically with increasing incidence. To take account of this it seems reasonable to replace $a_1/(a_1)_T$ in (14) by

$$\frac{C_L}{(C_L)_T} = \frac{C_L}{(a_1)_T(\alpha - \alpha_0)},$$

where α_0 is the no-lift angle.

Evidence from Refs. 13 and 14 points to the conclusion that the simplest relation approximately fitting the known facts for controls, whether balanced or unbalanced, is

$$\frac{b'}{(b')_T} = \frac{b_1}{(b_1)_T}.$$

More data* are needed before this relation can be accepted as established, but nothing better can be adopted on the available evidence fully discussed in Ref. 5.

TABLE 2

Theoretical values of b'/b_1 for a Thin Plate

λ	$(\lambda+1)E$									
	0·08	0·10	0·15	0·20	0·25	0·30	0·35	0·40	0·45	0·50
0	7·724	7·655	7·481	7·304	7·128	6·949	6·768	6·585	6·400	6·213
0·05	7·739	7·673	7·509	7·343	7·176	7·007	6·837	6·665	6·492	6·316
0·10	7·756	7·696	7·543	7·388	7·233	7·076	6·919	6·760	6·600	6·439
0·15	7·778	7·722	7·583	7·442	7·302	7·160	7·019	6·876	6·733	6·590
0·20	7·803	7·754	7·632	7·509	7·387	7·264	7·141	7·019	6·898	6·778
0·25	7·835	7·795	7·694	7·593	7·493	7·394	7·297	7·202	7·109	7·019

For a thin plate with unbalanced control ($\lambda = 0$), $(b')_T/(b_1)_T$ decreases slightly with increasing E. Table 2 also indicates a rather smaller increase in $(b')_T/(b_1)_T$ with increase of λ for balanced controls of the same total chord $(\lambda + 1)Ec$. But the variation with balance for a constant flap chord ratio E, based on the chord behind the hinge, is often negligible and only exceeds 4 per cent for very large controls with heavy balance. In the present uncertain state of knowledge it should normally suffice to use Table 2 in conjunction with

$$b' = b_1\left(\frac{b'}{b_1}\right)_T. \qquad \ldots\ldots\ldots\ldots\ldots\ldots\ldots \quad (15)$$

* Recent tests on a cambered wing—A.R.C. 15,456 (Garner and Batson, 1952)—confirm equations (14) and suggest in place of equation (15), $\frac{b'}{b_1} = \frac{(b')_{\text{thin-plate theory}}}{(b_1)_{\text{aerofoil theory}}}$.

To allow for compressibility a_1 and b_1 and therefore the camber derivatives, as defined in (14) and (15), need to be increased by the factor

$$\frac{1}{\beta} = \frac{1}{\sqrt{(1 - M^2)}} .$$

In the case of two-dimensional experiments the linear perturbation theory[18] (Goldstein and Young, 1943) shows that $(\Delta\alpha)$ and $(\Delta\gamma)$ in (9) also require a factor $1/\beta$.

The following procedure for determining tunnel-wall interference corrections to measurements on a two-dimensional wing in a closed subsonic rectangular tunnel is recommended:

(*a*) Apply the blockage correction (ΔV) to V [section 4.1 from (4)].

(*b*) Correct the measured incidence by the amount

$$(\Delta\alpha) = \frac{\pi}{48\beta}\left(\frac{c}{h}\right)^2 \{(C_L)_1(1 - 2l_1) + (C_L)_2(1 - 2l_2)\} .$$

(*c*) Correct the measured coefficients C_L', C_m', C_H' by respective amounts

$$\left.\begin{aligned} (\Delta C_L) &= -\frac{\pi a'}{192\beta}\left(\frac{c}{h}\right)^2 C_L' \\ (\Delta C_m) &= -\frac{\pi m'}{192\beta}\left(\frac{c}{h}\right)^2 C_L' \\ (\Delta C_H) &= -\frac{\pi b'}{192\beta}\left(\frac{c}{h}\right)^2 C_L' \end{aligned}\right| .$$

Of the quantities occurring in these expressions,

$(C_L)_1$ is the measured lift coefficient due to wing incidence,

l_1 is approximately $\frac{1}{4}$ and may be estimated more accurately from the correlated experimental data in Ref. 15 (1950),

$(C_L)_2$ is the additional measured lift coefficient due to a flap deflection, if any,

l_2 is given approximately by the theoretical values in (8) and Table 1, but should preferably be modified by an empirical correction factor of 1·07 (or estimated from Ref. 15),

$$a' = 4\pi\frac{a_1}{(a_1)_T}, \qquad m' = -\pi\frac{a_1}{(a_1)_T}, \qquad b' = b_1\left(\frac{b'}{b_1}\right)_T .$$

It should be noted that $(C_L)_1$ and $(C_L)_2$ are corrected for tunnel blockage. If the thickness/chord ratio of the wing is large b' should be modified in accordance with the footnote to (15). In the formulae for a' and m' it is sometimes important to replace $a_1/(a_1)_T$ by

$$\frac{a_1}{(a_1)_T}\frac{C_L'}{(a_1)'(\alpha' - \alpha_0') + (a_2)'\xi} ,$$

where α', α_0' are respectively the measured incidence and measured no-lift angle,

$(a_1)'$ is the value of $\dfrac{\partial C_L'}{\partial\alpha'}$, when α' is small,

$(a_2)'$ is the value of $\dfrac{\partial C_L'}{\partial\xi}$ corresponding to a small flap deflection ξ.

In instances of compressible flow, when a_1 and b_1 are not available from the tests themselves, it may be necessary to estimate their values from low-speed charts in Ref. 11, in order to determine the camber derivatives a', m' and b', given above. The values so obtained would require the compressibility factor $1/\beta$.

4.3. *Interference Corrections in Open-Jet Tunnels.*—On the assumptions that the boundary of an open jet is not influenced by the presence of the model and that the disturbance to the tunnel velocity at the boundary of the jet is small, Glauert[2] (1933) shows that the interference on a wing in a tunnel with a free boundary is determined by the following theorems :

(i) The interference on a small wing placed symmetrically in an open rectangular tunnel of breadth b parallel to the span and of height h is of the same magnitude as but of opposite sign to that on the same wing placed symmetrically in a closed tunnel of breadth h and height b.

(ii) The interference on any wing in an open circular tunnel is of the same magnitude as but of opposite sign to the of the same wing similarly placed in a closed tunnel of the same dimensions.

Unless the model is placed between end-plates and is of small chord the testing of a two-dimensional control surface in open-jet tunnels is considered to be valueless, for the initial assumptions are violated. Tunnel blockage will distort the jet boundary; and in an infinite free jet an additional interference arises on account of the downward deflection of the jet behind the wing. It is determined theoretically for a rectangular jet that for a typical value of $c/h = \frac{1}{3}$, there is a consequent correction to lift of nearly -40 per cent (Ref. 2, Fig. 21) and there are probably larger corrections to pitching and hinge moments. Moreover an open jet usually issues from a closed cylindrical mouth upstream of the model and enters a similar collector at moderate distance downstream. These conditions differ appreciably from those of an infinite free jet, and no experimental check on the reliability of the interference corrections is available.

For similar reasons, it is inadvisable to test large three-dimensional models in open-jet tunnels. If models are restricted to have spans not exceeding 0·6 of the tunnel breadth and chord not greater than 0·25 of the tunnel height it is probably accurate enough to use theorems (i), (ii) and the methods of section 4.4 and section 4.5 to determine the main interference correction, and to determine the blockage correction to V according to the final paragraph of section 4.1.

4.4. *Uniform Incidence or Full-Span Control.*—In problems of a complete wing inclined to the undisturbed stream or of a symmetrical tail model with a deflected full-span elevator, an elliptic distribution of lift is assumed*. The local centre of pressure is approximately represented by a constant value of l along the wing span.

If Λ is the angle of sweepback of the quarter-chord locus, for purposes of calculating wind-tunnel interference the wing is represented by a Vee lifting line swept back through an angle Λ_l given by

$$\tan \Lambda_l = \tan \Lambda - \frac{c_0}{s}(l - \tfrac{1}{4})(1 - \lambda) , \qquad (16)$$

where the taper parameter

$$\lambda = \frac{c_1}{c_0} = \frac{\text{tip chord}}{\text{root chord}} ,$$

which for wings of variable taper is conveniently generalised in the form

$$\lambda = \frac{4s}{Ac_0} - 1 .$$

The wing span is represented by $-s < t < s$. The lifting line is associated with an elliptically distributed circulation

$$\Gamma = \Gamma_0 \sqrt{\left[1 - \left(\frac{t}{s}\right)^2\right]} ,$$

which is accompanied by a wake of trailing vorticity of strength

$$K = \frac{d\Gamma}{dt}$$

per unit span.

* This assumption is justified in Appendix I.

The constraint of the tunnel walls on the flow due to this vorticity is equivalent to a distribution of upwash in the neighbourhood of the wing and may be evaluated from a system of images of the vorticity. As a basis of the calculation it is convenient to consider a single horse-shoe vortex of strength K and width $2t$, situated symmetrically in the tunnel with its lifting line at a position x_0. For small wings in incompressible flow, Glauert and Hartshorn[7] (1924) express the angle of upwash w/V, induced at a position x by the doubly infinite set of images in the tunnel walls, as

$$\frac{w}{V} = \frac{SC_L'}{C}\left\{\delta_0 + \frac{x - x_0}{h}\,\delta_1\right\}.$$

By extending this definition of δ_0 and δ_1, the angle of upwash, induced at (x, y) in the plane of the wing by the images of the single horse-shoe vortex, is

$$\frac{w}{V} = \frac{4Kt}{CV}\left\{\delta_0(y,t) + \frac{x - x_0}{h}\,\delta_1(y,t)\right\}, \qquad \ldots\ \ldots\ \ldots\ \ldots \quad (17)$$

where the quantities $\delta_0(y,t)$ and $\delta_1(y,t)$ may be calculated for closed tunnels by methods described in Appendix II.

Whatever the form of the working-section of a tunnel it is necessary that tables of $\delta_0(y,t)$ and $\delta_1(y,t)$ should be computed once for all. The ranges of y and t should cover all sizes of wing likely to be tested. In addition the tables might well include a similar set of values for wings placed, say, 6 inches above or below the central plane of the tunnel. When necessary $\delta_0(y,t)$ and $\delta_1(y,t)$ should be tabulated for both horizontal and vertical wing spans.

It is shown in Ref. 27, p. 4 (Acum, 1950) that under the conditions assumed for a swept wing in incompressible flow

$$\frac{w}{V} = \int_0^1 \frac{4\Gamma s}{CV}\left[\frac{\partial}{\partial t}\{t\delta_0(y,t)\} + \frac{x - x_0}{h}\,\frac{\partial}{\partial t}\{t\delta_1(y,t)\}\right] d\left(\frac{t}{s}\right), \qquad \ldots\ \ldots \quad (18)$$

where, measured from the leading edge of the root chord,

$$\begin{aligned} x_0 &= lc_0 + t\tan\Lambda_l \\ &= lc_0 + t\left\{\tan\Lambda - (l - \tfrac{1}{4})\left(\frac{2c_0}{s} - \frac{4}{A}\right)\right\} \text{ [from (16)]}. \qquad \ldots\ \ldots \quad (19) \end{aligned}$$

For the elliptic distribution of lift, Γ_0 is determined from the measured lift coefficient C_L' (corrected for tunnel blockage by the methods of section 4.1). Hence

$$\Gamma = \frac{VSC_L'}{\pi s}\sqrt{\left[1 - \left(\frac{t}{s}\right)^2\right]};$$

and it follows from (18) that in incompressible flow

$$\frac{w}{V} = \frac{4SC_L'}{\pi C}\int_0^1\left[\frac{\partial}{\partial t}\{t\delta_0(y,t)\} + \frac{x - x_0}{h}\,\frac{\partial}{\partial t}\{t\delta_1(y,t)\}\right]\sqrt{\left[1 - \left(\frac{t}{s}\right)^2\right]}\,d\left(\frac{t}{s}\right). \quad (20)$$

Subject to a linear chordwise variation of upwash, (20) will determine the angle of upwash, induced by wall interference, at any point (x,y) in the plane of the wing referred to the root leading edge. x_0, a function of t, has to be determined from (19), in which the only unknown is l. When the pitching moment is not measured, it is best to take

$$l = l_1 \text{ or } l_2 \quad \text{(section 4.2)}.$$

Otherwise the ratio C_m'/C_L' will determine an axis of zero pitching moment $x = \bar{x}$ and it is easy to equate this with the elliptic l-chord point. Thus

$$\bar{x} = \bar{c}\,.\,h_{\text{elliptic}} = c_0\left\{l + \frac{4}{3\pi}(1 - \lambda)(\tfrac{1}{4} - l) + \frac{4}{3\pi}\,\frac{s\tan\Lambda}{c_0}\right\};$$

i.e.,
$$l\left\{1 - \frac{4(1 - \lambda)}{3\pi}\right\} = \frac{\bar{x}}{c_0} - \frac{1 - \lambda}{3\pi} - \frac{4}{3\pi}\,\frac{s}{c_0}\tan\Lambda\,. \qquad \ldots\ \ldots\ \ldots\ \ldots \quad (21)$$

Using, if possible, the value of l from (21), it is simple to evaluate $\tan \Lambda_l$ as given in (19), and similarly

$$\tan \Lambda_{3/4} = \tan \Lambda - \left(\frac{c_0}{s} - \frac{2}{A}\right).$$

$\tan \Lambda_{3/4}$ is identically the tangent of the angle of sweepback of the three-quarter-chord locus for wings of uniform taper, and for the purposes of calculating tunnel interference it will normally suffice to take

$$x = \tfrac{3}{4}c_0 + y\left\{\tan \Lambda - \left(\frac{c_0}{s} - \frac{2}{A}\right)\right\} \quad .. \quad .. \quad .. \quad .. \quad .. \quad (22)$$

at the three-quarter chord of the section at y. Then in the notation of Ref. 27, the interference at this section is expressed as a local incidence at three-quarter chord and a local camber

$$\left.\begin{aligned} (\Delta\alpha)_{3/4} &= \frac{4SC_L'}{\pi sh} I \\ (\Delta\gamma) &= \frac{4SC_L'}{\pi sh}\frac{c}{8h} I_2 \end{aligned}\right\}, \quad .. \quad .. \quad .. \quad .. \quad .. \quad (23)$$

where $$I = I_1 + \left\{(\tfrac{3}{4} - l)\frac{c_0}{h} + \frac{y}{h}\tan \Lambda_{3/4}\right\} I_2 - \frac{b}{h}\tan \Lambda_l \,.\, I_3 ,$$

h is the height of the tunnel,

b is the breadth of the tunnel,

l is determined from (21), and

I_1, I_2 and I_3 are defined in Ref. 27, equations (4), (5) and (6),

viz.,

$$I_1 = \int_0^s \frac{\partial}{\partial t}\{(t\delta_0(y,t)\}\sqrt{\left[1 - \left(\frac{t}{s}\right)^2\right]}\frac{dt}{b} ;$$

$$I_2 = \int_0^s \frac{\partial}{\partial t}\{t\delta_1(y,t)\}\sqrt{\left[1 - \left(\frac{t}{s}\right)^2\right]}\frac{dt}{b} ;$$

$$I_3 = \int_0^s \frac{t}{b}\frac{\partial}{\partial t}\{t\delta_1(y,t)\}\sqrt{\left[1 - \left(\frac{t}{s}\right)^2\right]}\frac{dt}{b} .$$

Acum has calculated the spanwise distributions of $(\Delta\alpha)_{3/4}$ for elliptically loaded wings of various spans in rectangular tunnels in the case $l = \frac{1}{4}$. It is found from lifting-line theory (section 5.1) that for the purpose of estimating lift it is accurate enough to use a mean value of $(\Delta\alpha)_{3/4}$,

$$\begin{aligned} (\Delta\alpha) &= 0{\cdot}6 \text{ (elliptic mean)} + 0{\cdot}4 \text{ (chord mean)} \\ &= 0{\cdot}6\frac{\int_0^s (\Delta\alpha)_{3/4}\sqrt{\left[1 - \left(\frac{y}{s}\right)^2\right]}\,dy}{\int_0^s \sqrt{\left[1 - \left(\frac{y}{s}\right)^2\right]}\,dy} + 0{\cdot}4\,\frac{\int_0^s (\Delta\alpha)_{3/4}\,c\,dy}{\int_0^s c\,dy} \\ &= \int_0^1 (\Delta\alpha)_{3/4}\left\{\frac{2{\cdot}4}{\pi}\sqrt{\left[1 - \left(\frac{y}{s}\right)^2\right]} + \frac{0{\cdot}8cs}{S}\right\} d\left(\frac{y}{s}\right) \\ &= \frac{SC_L'}{C}\,.\,\delta , \quad .. \quad .. \quad .. \quad .. \quad .. \quad .. \quad .. \quad .. \quad (24) \end{aligned}$$

where δ is unexpectedly insensitive to changes in taper and sweep and is virtually dependent on aspect ratio, A, and span $\sigma = s/b$.

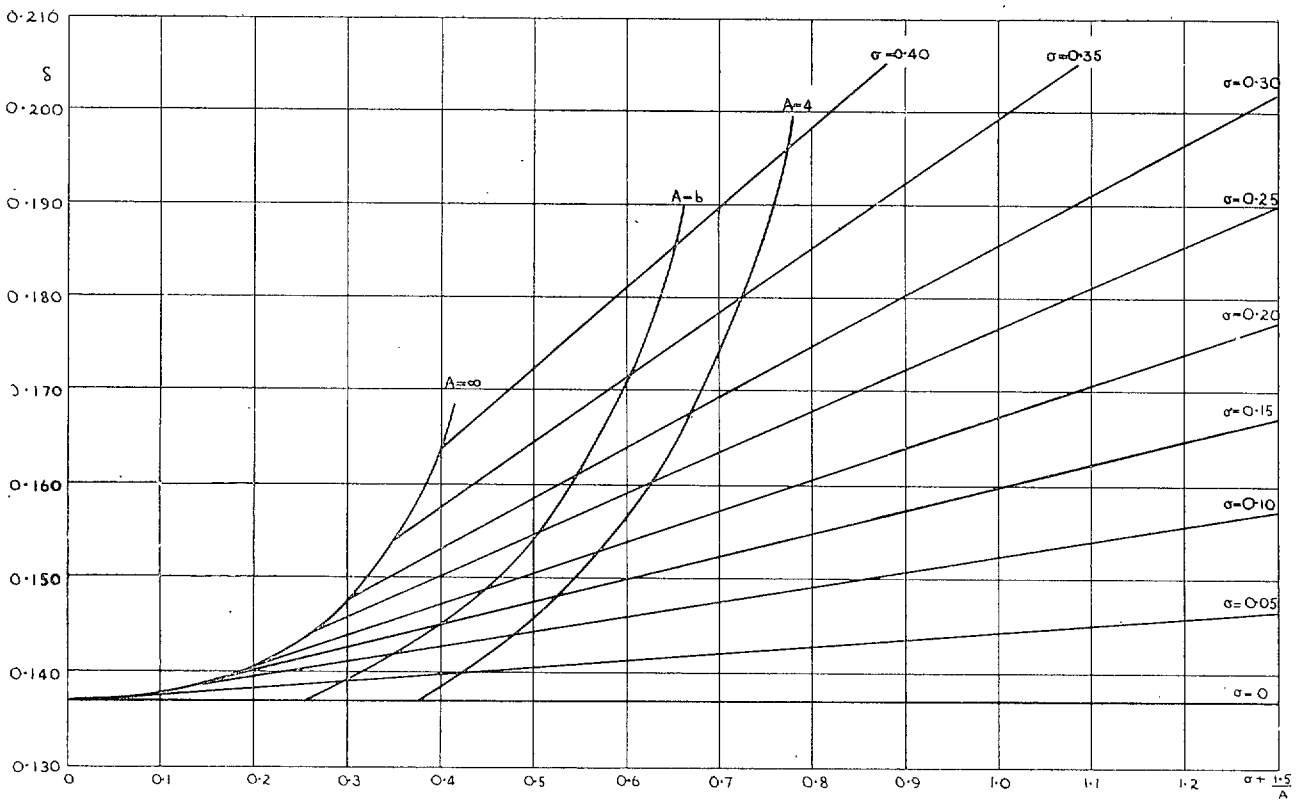

FIG. 2. δ against $(\sigma + 1{\cdot}5/A)$. Square tunnel.

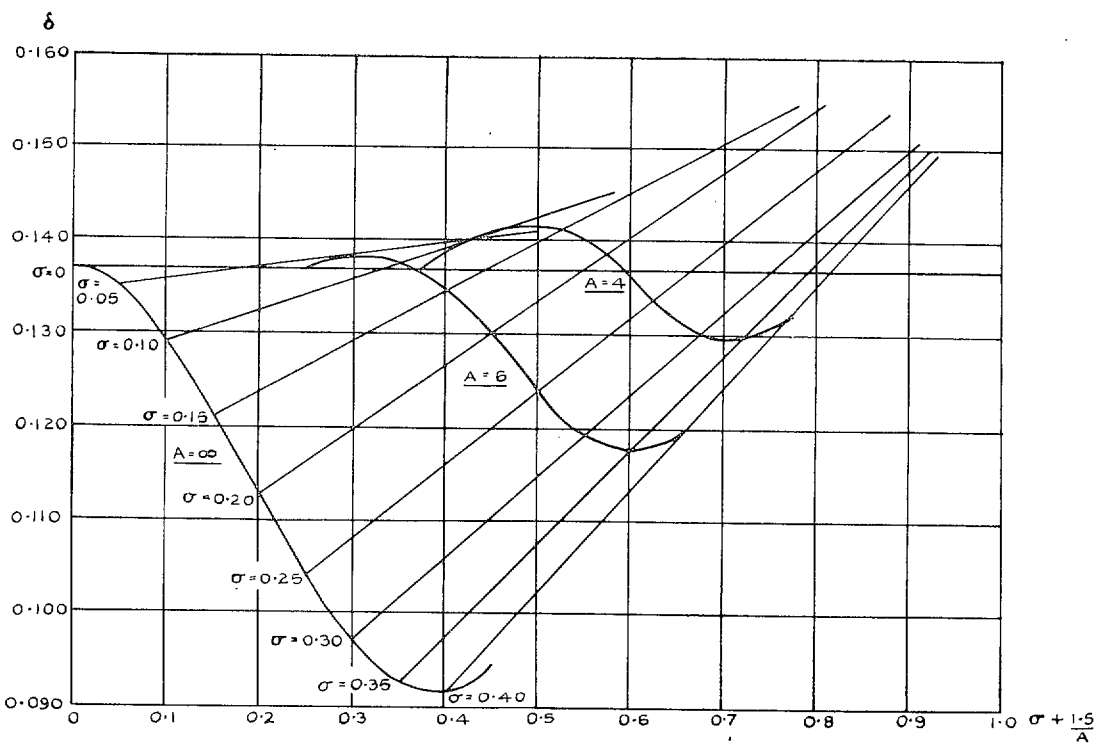

FIG. 3. δ against $(\sigma + 1{\cdot}5/A)$. Duplex tunnel $(b = 2h)$.

The values of δ are conveniently plotted against $(\sigma + 1{\cdot}5/A)$. Curves from Ref. 27 are reproduced in this report as follows:

Fig. 2. Square tunnel

Fig. 3. Duplex tunnel ($b = 2h$).

It is suggested that similar sets of curves* should be calculated for a representative series of tunnel working-sections. It will readily be seen that these curves can be applied to a more general case in which l is different from $\frac{1}{4}$ by substituting

$$\sigma + \frac{3}{A}\left(\tfrac{3}{4} - l\right)$$

in place of the abscissa $(\sigma + 1{\cdot}5/A)$. In this way δ in (24) may be evaluated with good accuracy for complete wings at a uniform incidence or with full-span controls and for a symmetrical tail model with a deflected full-span elevator.

In the theory of interference for a small wing represented by a single doublet vortex (Ref. 2, p. 21) the parameter δ is equaivalent to

$$\delta = \delta_0 + \delta_1\left(\tfrac{3}{4} - l\right)\frac{\bar{c}}{h},$$

and the induced camber is

$$(\Delta\gamma) = \frac{SC_L'}{C} \cdot \frac{\bar{c}}{8h} \cdot \delta_1 \qquad (25)$$

As an indication of the effect of tunnel cross-section, δ_0 and δ_1 are given in the following table.

TABLE 3

Interference for a Small Wing

Shape of tunnel	δ_0	δ_1	Reference
Square	0·137	0·240	7
Duplex (horizontal wing)	0·137	$0{\cdot}292_5$	7
Duplex (vertical wing)	0·262	0·512	2
Circular	0·125	0·250	25
Elliptical ($b/h = 1{\cdot}795$)	$0{\cdot}121_5$	0·291†	2
Rectangular 9 ft × 7 ft	0·120	$0{\cdot}228_5$	8
N.P.L. 9 ft × 7 ft with fillets	0·114	0·217†	8
Rectangular 13 ft × 9 ft	0·119	0·233	8
N.P.L. 13 ft × 9 ft with fillets	$0{\cdot}112_5$	0·220†	8

To the accuracy of the linear perturbation theory[18], δ_0 is unaffected by compressibility but δ_1 is subject to the correction factor

$$\frac{1}{\beta} = \frac{1}{\sqrt{(1 - M^2)}}.$$

* Similar curves for rectangular tunnels ($b = 9h/7$, $18h/7$) are included in Ref. 27.

† Denotes an estimated value. For the elliptical tunnel δ_1 is obtained by making an assumption similar to that in Ref. 2, p. 37. A ratio correction is also used to assess the influence of triangular fillets on δ_1 (Ref. 9).

Then, to summarise, in all problems in which the spanwise loading is approximately elliptic, the tunnel interference due to vorticity is expressed as a distribution of angle of upwash as in (20)

$$\frac{w}{V} = \frac{4SC_L'}{\pi C}\int_0^1 \left[\frac{\partial}{\partial t}\{t\delta_0(y,t)\} + \frac{x-x_0}{\beta h}\frac{\partial}{\partial t}\{t\delta_1(y,t)\}\right]\sqrt{\left[1-\left(\frac{t}{s}\right)^2\right]}\,d\left(\frac{t}{s}\right),$$

where x_0 is given in (19). At any section y the distribution of w/V is represented as

$$\left.\begin{aligned}(\Delta\alpha)_{3/4} &= \frac{4SC_L'}{\pi s h}\,I\\ (\Delta\gamma) &= \frac{4SC_L'}{\pi s h}\,\frac{c}{8h}\,\frac{1}{\beta}\,I_2\end{aligned}\right\},$$

where

$$I = I_1 + \left\{(\tfrac{3}{4}-l)\frac{c_0}{h} + \frac{y}{h}\tan\Lambda_{3/4}\right\}\frac{1}{\beta}\,I_2 - \frac{b}{\beta h}\tan\Lambda_l\,.\,I_3$$

and I_1, I_2, I_3 are defined in Ref. 27 and evaluated for rectangular tunnels ($b = h$, $9h/7$, $2h$, $18h/7$), and l is given in (21) or else by two-dimensional considerations (section 4.2). Finally

$$(\Delta\alpha) = \frac{SC_L'}{C}\,\delta$$

is evaluated as in (24). For square and duplex tunnels δ is given in Figs. 2 and 3 respectively (reproduced from Ref. 27). If the abscissa is replaced by

$$\sigma + \frac{3}{A\beta}(\tfrac{3}{4}-l)\,,$$

the value of δ corresponding to a given σ will take account of compressibility and any departure from $l = \frac{1}{4}$.

The correction $(\Delta\alpha)$ is applied as an increment to the incidence of test. In view of (24) there is no further correction to the measured lift. There is a small residual correction to the measured pitching moment; this is shown to be small, independent of pitching axis, and difficult to compute (Ref. 27). When the procedure of this section is adopted the residual (ΔC_m) may usually be neglected for small values of σ. The residual (ΔC_H) to be added to the measured hinge-moment coefficient should always be included; practical methods of estimating these incremental corrections are given in section 4.5, equations (32) and (33).

In undertaking calculations for a new tunnel, the first step is to evaluate the quantities $\delta_0(y,t)$ and $\delta_1(y,t)$ once for all by the methods suggested in Appendix II. For rectangular tunnels the summation in series obtained by Olver[28] (1949) is of assistance. The second step is to carry out the calculations fully described in Ref. 27 and finally to produce curves in the convenient form of Figs. 2 and 3.

4.5. *Deflected Partial-Span Control.*—The method of section 4.4 for evaluating the upwash due to tunnel interference is not applicable when the model under test has deflected control surfaces of partial span. In the first place the spanwise wing loading is not elliptic and further the local centre of pressure is not truly represented by a constant value of l along the wing span.

Take for instance the problem of a half-wing with a deflected aileron of span

$$y_1 < y < y_0$$

mounted on one wall of a tunnel. An unswept example of this has been considered in detail in connection with the work of Ref. 17. The whole wing with symmetrical ailerons is imagined

to be placed symmetrically in a tunnel of the same height and twice the breadth. The disturbance to the tunnel stream is satisfactorily represented by two discrete horse-shoe vortices:

(i) of strength K_0 and span $2y_0$ with its bound vortex at a constant chordwise position l_0c to be determined from the pitching moment,

(ii) of strength $-K_1$ and span $2y_1$ with its bound vortex at $0{\cdot}3c$ from the leading edge.

This assumption presupposes a total lift on the half wing

$$L = \rho V(K_0y_0 - K_1y_1)$$

and a total rolling moment

$$\mathscr{L} = \tfrac{1}{2}\rho V(K_0y_0^2 - K_1y_1^2) .$$

If both lift and rolling moment are measured these will determine K_0 and K_1. If, however, only rolling moment is measured, then the spanwise centre of pressure $\bar{y}$ must be estimated (section 5.2). Thus

$$\frac{K_0}{K_1} = \frac{y_1}{y_0}\frac{2\bar{y} - y_1}{2\bar{y} - y_0}$$

and their magnitudes are determined by the measured rolling moment. If the pitching moment is not measured, it is best to take $l_0c = l_2c$, the chordwise centre of pressure for a two-dimensional flap (Table 1). For an unswept wing the distribution of upwash is calculated at once from (17). In the notation of (23)

$$\left.\begin{aligned}(\Delta\alpha)_{3/4} &= \frac{4K_0y_0}{CV}\left\{\delta_0(y,y_0) + \frac{c}{\beta h}(\tfrac{3}{4} - l_2)\delta_1(y,y_0)\right\} \\ &\quad - \frac{4K_1y_1}{CV}\left\{\delta_0(y,y_1) + \frac{c}{\beta h}(0{\cdot}45)\delta_1(y,y_1)\right\} \\ (\Delta\gamma) &= \frac{K_0y_0}{2C\bar{V}}\cdot\frac{c}{\beta h}\,\delta_1(y,y_0) - \frac{K_1y_1}{2C\bar{V}}\frac{c}{\beta h}\,\delta_1(y,y_1)\end{aligned}\right\}, \qquad \ldots \quad (26)$$

where $\delta_0(y,y_0)$, $\delta_1(y,y_0)$, $\delta_0(y,y_1)$, $\delta_1(y,y_1)$ should be available in tabular form, and the factor β allows for compressibility.

A rapid procedure of this kind is needed for swept wings and it is suggested that the same assumptions (i) and (ii) should be used. The vorticity now corresponds to two uniformly loaded lifting lines swept respectively through angles Λ_0 and Λ_1, obtained by substituting the appropriate values of l in (16):

$$\left.\begin{aligned}\tan\Lambda_0 &= \tan\Lambda - (l_0 - \tfrac{1}{4})\left(\frac{2c_0}{s} - \frac{4}{A}\right) \\ \tan\Lambda_1 &= \tan\Lambda - 0{\cdot}05\left(\frac{2c_0}{s} - \frac{4}{A}\right)\end{aligned}\right\}.$$

This configuration implies a pitching moment on the half-wing

$$-\mathscr{M} = \rho VK_0y_0(l_0c_0 + \tfrac{1}{2}y_0\tan\Lambda_0) - \rho VK_1y_1(0{\cdot}3c_0 + \tfrac{1}{2}y_1\tan\Lambda_1)$$

about an axis through the leading apex and a chordwise centre of pressure at $x = \bar{x}$ given by

$$\bar{x}(K_0y_0 - K_1y_1) = K_0y_0(l_0c_0 + \tfrac{1}{2}y_0\tan\Lambda_0) - K_1y_1(0{\cdot}3c_0 + \tfrac{1}{2}y_1\tan\Lambda_1) .$$

When $\bar{x}$ is known experimentally,

$$(l_0 - 0{\cdot}3)\left\{c_0 - \tfrac{1}{2}y_0\left(\frac{2c_0}{s} - \frac{4}{A}\right)\right\} = (\bar{x} - 0{\cdot}3c_0)\left(1 - \frac{K_1y_1}{K_0y_0}\right) - \tfrac{1}{2}y_0\tan\Lambda_1\left(1 - \frac{K_1y_1^2}{K_0y_0^2}\right). \quad (27)$$

Otherwise $l_0 = l_2$ should be used. Then the upwash calculated from (18) and (19) is

$$\begin{aligned}\frac{w}{V} &= \frac{4K_0}{CV}\int_0^{y_0}\left[\frac{\partial}{\partial t}\{t\delta_0(y,t)\} + \frac{x - l_0c_0 - t\tan\Lambda_0}{\beta h}\frac{\partial}{\partial t}\{t\delta_1(y,t)\}\right]dt \\ &\quad - \frac{4K_1}{CV}\int_0^{y_1}\left[\frac{\partial}{\partial t}\{t\delta_0(y,t)\} + \frac{x - 0\cdot3c_0 - t\tan\Lambda_1}{\beta h}\frac{\partial}{\partial t}\{t\delta_1(y,t)\}\right]dt \\ &= \frac{4K_0y_0}{CV}\left\{\delta_0(y,y_0) + \frac{x - l_0c_0}{\beta h}\delta_1(y,y_0)\right\} \\ &\quad - \frac{4K_1y_1}{CV}\left\{\delta_0(y,y_1) + \frac{x - 0\cdot3c_0}{\beta h}\delta_1(y,y_1)\right\} \\ &\quad - \frac{4K_0\tan\Lambda_0}{CV\beta h}\int_0^{y_0}\frac{\partial}{\partial t}\{t\delta_1(y,t)\}t\,dt \\ &\quad + \frac{4K_1\tan\Lambda_1}{CV\beta h}\int_0^{y_1}\frac{\partial}{\partial t}\{t\delta_1(y,t)\}t\,dt\,.\end{aligned}$$

Therefore

$$\begin{aligned}\frac{w}{V} &= \frac{4K_0y_0}{CV}\left\{\delta_0(y,y_0) + \frac{x - l_0c_0 - y_0\tan\Lambda_0}{\beta h}\delta_1(y,y_0)\right\} \\ &\quad - \frac{4K_1y_1}{CV}\left\{\delta_0(y,y_1) + \frac{x - 0\cdot3c_0 - y_1\tan\Lambda_1}{\beta h}\delta_1(y,y_1)\right\} \\ &\quad + \frac{4K_0\tan\Lambda_0}{CV\beta h}\int_0^{y_0}t\delta_1(y,t)\,dt - \frac{4K_1\tan\Lambda_1}{CV\beta h}\int_0^{y_1}t\delta_1(y,t)\,dt\,. \qquad \ldots\ \ \ldots \quad (28)\end{aligned}$$

Thus for swept-back wings the interference at a section y is given by

$$\left.\begin{aligned}(\Delta\alpha)_{3/4} &= \frac{w}{V} \text{ from (28) putting} \\ x &= \tfrac{3}{4}c_0 + y\left\{\tan\Lambda - \left(\frac{c_0}{s} - \frac{2}{A}\right)\right\} \text{ as in (22)} \\ (\Delta\gamma) &= \frac{K_0y_0}{2CV}\frac{c}{\beta h}\delta_1(y,y_0) - \frac{K_1y_1}{2CV}\frac{c}{\beta h}\delta_1(y,y_1) \text{ as in (26)}\end{aligned}\right\} \ldots\ \ \ldots\ \ \ldots \quad (29)$$

The computation of $\delta_0(y,t)$ and $\delta_1(y,t)$ is discussed in Appendix II. The numerical evaluation of the two integrals in (28) for any given value of y is easily carried out by Simpson's Rule (or its equivalent if y_0 and y_1 differ from the values of t for which $\delta_1(y,t)$ is computed).

The method of evaluating $(\Delta\alpha)_{3/4}$ and $(\Delta\gamma)$ in the case of ailerons of partial span can obviously be extended to include deflected inboard flaps, which may be regarded as the difference between a full-span flap treated in section 4.4 and the aileron considered here.

Having computed $(\Delta\alpha)_{3/4}$ and $(\Delta\gamma)$ from (26) or (29), the mean value from (24)

$$(\Delta\alpha) = 0\cdot6\{\text{elliptic mean of } (\Delta\alpha)_{3/4}\} + 0\cdot4\{\text{chord mean of } (\Delta\alpha)\}_{3/4}$$

is first applied as a correction to the incidence of test. The residual tunnel interference is then expressed as a local incidence at mid-chord and a local camber

$$\left.\begin{aligned}(\delta\alpha) &= (\Delta\alpha)_{3/4} - 2(\Delta\gamma) - (\Delta\alpha) \\ (\delta\gamma) &= (\Delta\gamma)\end{aligned}\right\} \ldots\ \ \ldots\ \ \ldots\ \ \ldots\ \ \ldots\ \ \ldots \quad (30)$$

For special accuracy it is necessary to use the method described in section 4.6 to obtain the increments

$$(\Delta C_L),\ (\Delta C_l),\ (\Delta C_m),\ (\Delta C_H)$$

to the measured C_L', C_l', C_m', C_H', when the extraneous flow represented in (30) is removed. When the simplifying assumptions of sections 4.4. and 4.5 are involved in obtaining $(\delta\alpha)$ and $(\delta\gamma)$, the authors do not consider that elaborate calculations are demanded. By the definition of $(\Delta\alpha)$ in (24) it is presumed that there is no further correction (ΔC_L). Thus (ΔC_m) is independent of the pitching axis.

The following simple formulae should be used:

$$*(\Delta C_l) = -\frac{\partial C_l}{\partial\alpha}\int_0^s\{(\Delta\alpha)_{3/4} - (\Delta\alpha)\}cy\sqrt{(s^2-y^2)}\,dy \Big/ \int_0^s cy\sqrt{(s^2-y^2)}\,dy \quad .. \quad (31)$$

$$(\Delta C_m) = -A\tan\Lambda\,(\Delta C_l) - m'\cos\Lambda\int_0^s\left(\frac{c}{\bar{c}}\right)^2(\delta\gamma)\frac{dy}{s} \quad .. \quad .. \quad .. \quad (32)$$

$$(\Delta C_H) = -\frac{\partial C_H}{\partial\alpha}\int_{y_1}^{y_0}\left\{(\delta\alpha) + \frac{b'}{b_1}(\delta\gamma)\right\}c_f^2\sqrt{(s^2-y^2)}\,dy \Big/ \int_{y_1}^{y_0} c_f^2\sqrt{(s^2-y^2)}\,dy\,, \quad .. \quad (33)$$

where $(\delta\alpha)$ and $(\delta\gamma)$ are defined in (30).

In (31) (*see* footnote), $\partial C_l/\partial\alpha$ is the experimental derivative of the rolling-moment coefficient corrected to free-stream conditions. It is sufficient to use the value

$$\frac{\partial C_l'}{\partial\{\alpha' + (\Delta\alpha)\}}$$

where α' is the measured incidence of test, $(\Delta\alpha)$ is determined from section 4.4 and C_l' is the measured rolling-moment coefficient, corrected for tunnel blockage (section 4.1).

(ΔC_m) consists of two contributions:

(i) the pitching moment about an axis through the root quarter-chord corresponding to the residual spanwise distributions of lift concentrated on the quarter-chord locus

(ii) the additional moment from the residual camber on the basis of two-dimensional strip theory, the camber derivative m' being given in (14) and requiring a factor $1/\beta$ for compressibility.

In (33), it is sufficient to use

$$\frac{\partial C_H}{\partial\alpha} = \frac{\partial C_H'}{\partial\{\alpha' + (\Delta\alpha)\}}.$$

The ratio b'/b_1 is given in Table 2 (section 4.2).

The formulae (31), (32) and (33) are likely to be in error by $\pm$ 25 per cent. However these residual corrections will usually be small enough for this not to matter.

To summarise, for many three-dimensional experiments, including all *ad hoc* work, the corrections for interference may be calculated in the following stages:

(*a*) Correct the speed of test for tunnel blockage (section 4.1) and compute the aerodynamic coefficients

e.g., C_L', C_l', C_m', C_H'

from tunnel measurements.

---

* Equation (31) gives the correction to the rolling moment measured on a half-wing. $\partial C_l/\partial\alpha$ has a meaning if it is interpreted in the sense of equation (40).

(*b*) Use the expressions in equations

(23) for uniform incidence or full-span controls

(29) for deflected controls of partial span

to compute $(\Delta\alpha)_{3/4}$ and $(\Delta\gamma)$ at a suitable number of spanwise positions.

(*c*) Evaluate $(\Delta\alpha)$ from equation (24) and apply it as a correction to the incidence of test.

(*d*) Evaluate (ΔC_l), (ΔC_m), (ΔC_H), as may be required, from the respective equations (31), (32), (33), and add these quantities to the corresponding coefficients in (*a*).

4.6. *Accurate Determination of Tunnel Interference for a Large Model.*—Experience suggests that the methods of the previous section for the estimation of wall interference corrections may not always be accurate enough for really large models, particularly when pitching and hinge moments are the measurements to be corrected. The following procedure is fairly simple to apply to special tests although too elaborate for frequent use. It makes use of the lifting-surface theory[10], which has improved the accuracy in calculating the distribution of load or circulation along the span of a finite wing with partial span controls*. For determining wind-tunnel interference this 'lifting-surface' circulation Γ is associated with the representative 'lifting-line' through the local centres of pressure. Then the expression for the induced angle of upwash in (18) becomes

$$\frac{w}{V} = \int_0^s \frac{4\Gamma}{C\overline{V}} \left\{ \frac{\partial}{\partial t}\{t\delta_0(y,t)\} + \frac{x - R(t) + (\tfrac{1}{2} - l)c(t)}{\beta h} \frac{\partial}{\partial t}\{t\delta_1(y,t)\} \right\} dt , \qquad .. \quad (34)$$

where $x = R(y)$ is the locus of mid-chord points,

$x = R(t) + (l - \tfrac{1}{2})c(t)$ is the equation of the lifting line,

$\beta = \sqrt{(1 - M^2)}$ is the factor for compressibility.

It is shown in Appendix I that, for a given measured C_L', the calculation of tunnel interference does not require the spanwise distribution of lift to great accuracy. It is sufficient to use estimated free-stream distributions of Γ corresponding to the measured C_L' (section 5.1). The local interference at any wing section is obtained by substituting estimated values of l and calculated distributions of Γ in (34). Hence, from formulae analogous to (29), the quantities $(\Delta\alpha)_{3/4}$ and $(\Delta\gamma)$ may be evaluated at any section. The incremental circulation $(\delta\Gamma)$ corresponding to the local incidence $(\Delta\alpha)_{3/4}$ is then calculated by means of section 5.1; and its contributions to lift and rolling moment (δC_L) and (δC_l) are obtained by substituting $\Gamma = (\delta\Gamma)$ in (40).

The form in which the main interference correction is applied is to some extent arbitrary. No difficulty arises when the curves of measured lift and rolling moment are linear with incidence; for either $-(\delta C_L)$ and $-(\delta C_l)$ may be applied as corrections to the measured coefficients C_L' and C_l' or an equivalent correction may be applied to the incidence. The former procedure may be preferred in correcting control derivatives; but for all other purposes it is satisfactory to use a correction to the incidence of test. When serious turbulent separation is present, the conditions of test are best represented when the major correction for tunnel interference takes the form of an increment of incidence equal to a mean upwash angle in the tunnel. This is conveniently chosen to be

$$(\Delta\alpha) = (\delta C_L) \Big/ \frac{\partial C_L}{\partial\alpha} . \qquad .. \quad .. \quad .. \quad .. \quad .. \quad .. \quad (35)$$

Then the measured lift applies to free-stream conditions. But there remains a supplementary correction

$$(\Delta C_l) = -\{(\delta C_l) - (\Delta\alpha)\,\partial C_l/\partial\alpha\}; \qquad .. \quad .. \quad .. \quad .. \quad (36)$$

and it is necessary to allow for residual interference due to induced curvature of flow and to the spanwise variation of upwash angle. On the basis of equation (34), $(\delta\alpha)$ and $(\delta\gamma)$ in (30)

* Ref. 10 has been superseded by R. & M. 2884 (Multhopp, 1950), which deals with sweepback.

should be calculated. Then, (ΔC_l) being known, the formulae (32) and (33) for (ΔC_m) and (ΔC_H) are recommended. At high incidence the necessary derivatives may not be known with any certainty, but they can usually be estimated well enough for the purpose of making these comparatively small corrections.

5. *Free-Stream Calculations.*—The method of tunnel interference correction, which has just been outlined, involves a procedure for estimating forces and moments under free-stream conditions by using an approximate theory. This same calculation is often appropriate for giving a satisfactory indication of the corrections for Reynolds number (section 6) to be applied to the free-stream values deduced from the tunnel measurements by the methods of the preceding paragraphs.

Since the preparation of this report a satisfactory theoretical method of treating a swept wing with partial-span controls has appeared (R. & M. 2884 (Multhopp, 1950)). This subsonic lifting-surface theory should be used in preference to the approximate procedure which follows. However sections 5.1 and 5.2 describe a more rapid method of calculation and a means of allowing for sectional characteristics not inherent in the theory.

5.1. *Lifting-Line Theory.*—The spanwise distribution of circulation Γ round a wing with deflected controls in a uniform free stream may be calculated from the lifting-line theory, as developed by Multhopp[12] (1938). In calculations for compressible flow the lateral dimensions of the wing should be reduced so that the semi-span becomes βs. For the application of Multhopp's method it is necessary to use the chord c, the lift slope and the equivalent incidence $[\alpha + (a_2/a_1)\xi]$ at certain wing sections. a_1 and a_2 may be estimated by the process described in Ref. 11. For swept wings they should both be modified by the factor $\cos \Lambda'$ from equation (44).

Let the reduced spanwise distance from the wing root be $\beta y = \beta s \cos \phi$; then Multhopp chooses stations

$$\phi = \phi_\nu = \frac{\nu\pi}{m+1} \qquad (\nu = 1, 2, 3, \ldots \tfrac{1}{2}(m+1))$$

along the semi-span. A continuous and symmetrical distribution of equivalent incidence can be represented by its values α_ν at the selected stations. The computation then amounts to the solution of $\frac{1}{2}(m+1)$ linear simultaneous equations, from which the circulation Γ_ν at each station can be expressed conveniently in non-dimensional form

$$\frac{\Gamma_\nu}{2sV} = \sum_{n=1}^{\frac{1}{2}(m+1)} D_{\nu n}\alpha_n \,. \qquad \ldots \qquad (37)$$

The factors $D_{\nu n}$ depend only on the $\frac{1}{2}(m+1)$ values of $(c/4\beta s)a_1 \cos \Lambda'$ and m, which is usually 7 or 15. Thus the calculation is identically that for the actual wing of semi-span s with a lift slope $(1/\beta)a_1 \cos \Lambda'$ in place of the value a_1 for an unswept wing of the same section in incompressible flow.

When a partial-span control is deflected, the equivalent incidence has discontinuities at the ends of the control. Multhopp's method treats the integral equation of the lifting-line by prescribing equal and opposite discontinuities in the induced incidence, which determines a circulation $(\Gamma_\nu)_{\mathrm{I}}$ (Ref. 12, section VII). Thereby the problem is reduced to one with a residual continuous distribution of incidence $(\alpha_n)_{\mathrm{II}}$, for which equation (37) determines the corresponding circulation $(\Gamma_\nu)_{\mathrm{II}}$. Then

$$\Gamma_\nu = (\Gamma_\nu)_{\mathrm{I}} + (\Gamma_\nu)_{\mathrm{II}} \,. \qquad \ldots \qquad (38)$$

The coefficients of lift and rolling moment are then given by

$$\left.\begin{aligned} C_L &= \frac{\pi A}{m+1} \sum_1^m \frac{\Gamma_\nu}{2sV} \sin \phi_\nu \\ C_l &= \frac{\pi A}{4(m+1)} \sum_1^m \frac{\Gamma_\nu}{2sV} \sin 2\phi_\nu \end{aligned}\right\}, \qquad \ldots \qquad (39)$$

where $\phi_\nu = \nu\pi/(m+1)$. This applies to a complete wing.

For a half-wing with a symmetrical distribution of lift about the root chord,

$$\left.\begin{aligned} C_L &= \frac{2\pi A}{m+1}\left[\sum_1^{\frac{1}{2}(m-1)}\left(\frac{\Gamma_\nu}{2sV}\sin\phi_\nu\right)+\tfrac{1}{2}\,\frac{\Gamma_{\frac{1}{2}(m+1)}}{2sV}\right] \\ C_l &= \frac{A}{2}\int_0^{\pi/2}\frac{\Gamma}{2sV}\sin 2\phi\,d\phi = \frac{\pi A}{m+1}\sum_1^{\frac{1}{2}(m+1)}\left(F_\nu\frac{\Gamma_\nu}{2sV}\right) \end{aligned}\right\}, \quad .. \quad .. \quad (40)$$

where F_ν is given below:

m	F_1	F_2	F_3	F_4	F_5	F_6	F_7	F_8
7	0·3525	0·5030	0·3440	0·0404	—	—	—	—
15	0·1913	0·3637	0·4617	0·5004	0·4612	0·3552	0·1867	0·0200

There is no need to refine these solutions for the purpose of calculating the tunnel interference. Values of the circulation from (38) should be associated with estimated local centres of pressure and used in accordance with section 4.6. The local interference $(\Delta\alpha)_{3/4}$ and $(\Delta\gamma)$ corresponding to this assumed wing loading should of course be adjusted in the ratio

$$\frac{\text{measured } C_L' \text{ (corrected for blockage)}}{\text{calculated } C_L \text{ from (38) and (39)}}.$$

The correction to the measured incidence, defined in (35), is the mean value of $(\Delta\alpha)_{3/4}$ found by substituting $\alpha = (\Delta\alpha)_{3/4}$ and $\alpha = 1$ in equation (37) and the values of Γ so obtained in (39), *viz.*,

$$(\Delta\alpha) = \frac{\sum_{\nu=1}^{m}\left[\sum_{n=1}^{\frac{1}{2}(m+1)} D_{\nu n}(\Delta\alpha_n)_{3/4}\right]\sin\dfrac{\nu\pi}{m+1}}{\sum_{\nu=1}^{m}\left[\sum_{n=1}^{\frac{1}{2}(m+1)} D_{\nu n}\right]\sin\dfrac{\nu\pi}{m+1}}, \quad .. \quad .. \quad .. \quad .. \quad (41)$$

where $(\Delta\alpha_n)_{3/4}$ is the value of $(\Delta\alpha)_{3/4}$ at the station $y = s\cos\{n\pi/(m+1)\}$. The residual corrections to C_l, C_m, C_H then follow from the procedure in section 4.6. In particular*, from (36)

$$(\Delta C_l) = \frac{\partial C_l}{\partial\alpha}\left\{(\Delta\alpha) - \frac{\sum_{\nu=1}^{\frac{1}{2}(m+1)} F_\nu\left[\sum_{n=1}^{\frac{1}{2}m+1} D_{\nu n}(\Delta\alpha_n)_{3/4}\right]}{\sum_{\nu=1}^{\frac{1}{2}(m+1)} F_\nu\left[\sum_{n=1}^{\frac{1}{2}(m+1)} D_{\nu n}\right]}\right\}, \quad .. \quad .. \quad .. \quad (42)$$

where $\partial C_l/\partial\alpha$ is the corrected experimental coefficient of rolling moment on the half-wing, as defined in (40).

The lifting-line theory is applicable to problems with asymmetrical spanwise loading. Symmetrical and antisymmetrical parts are conveniently separated so that, when antisymmetrical ailerons are considered, an independent calculation is required. The treatment resembles that in the symmetrical case (Ref. 12, section VII); and the same modified two-dimensional lift slope $(1/\beta)a_1\cos\Lambda'$ should be used.

5.2. *Practical Correlation.*—When allowing for a change of Reynolds number or Mach number, some correlation between the measured and calculated coefficients is desirable. The free-stream calculations of section 5.1 should be carried out for two extreme values of $(1/\beta)a_1\cos\Lambda'$ consistent with the range of boundary-layer transition, Reynolds number and Mach number. Some corrections to the lifting-line theory should then be applied.

* When R. & M. 2884 is used, (ΔC_m) and (ΔC_H) may be evaluated from equations similar to (42).

To evaluate the lift slope $(a_1)_{\text{l.l.}}$ for an unswept wing in incompressible flow, the procedure of section 5.1 may be bypassed with the aid of the approximate formula (Glauert; Ref. 19, Chapter 11)

$$\frac{A}{(a_1)_{\text{l.l.}}} = \frac{A}{a_1} + \frac{1+\tau}{\pi}, \qquad \text{(43)}$$

where τ is a function of A/a_1, and the taper parameter

$$\lambda = \frac{c_1}{c_0} = \frac{\text{tip chord}}{\text{root chord}} = \left\{\frac{4s}{Ac_0} - 1\right\} \text{ for wings of variable taper.}$$

Since the lifting-line theory makes no allowance for sweepback or the induced curvature of flow associated with finite chord, it is necessary to modify (43) to include these effects and compressibility. Low-speed experiments at the N.P.L. have given values of $\partial C_L/\partial\alpha$ rather closer to $(a_1)_{\text{l.l.}}$ than the predictions of lifting-surface theory have suggested. For wings of moderate aspect ratio the authors recommend the practical formula

$$\frac{\partial C_L}{\partial \alpha} = (a_1)_{\text{eff.}} = A\left\{\frac{1}{p} + \frac{1+\tau}{\pi} + 0{\cdot}032\sqrt{p}\right\}^{-1}, \qquad \text{(44)}$$

where

$$p = \frac{1}{\beta A} a_1 \cos \Lambda',$$

$$\tan \Lambda' = \left\{1 - \frac{0{\cdot}8}{\beta A(\lambda+1)}\right\} \frac{1}{\beta} \tan \Lambda,$$

Λ is the angle of sweepback of the quarter-chord locus,

$$\tau = f(\lambda) \,.\, g\left(\frac{1}{p}\right),$$

where f and g are given approximately in the respective Tables 4A and 4B.

Thus $(a_1)_{\text{eff.}}$ may be evaluated for the two extreme values of $(1/\beta)a_1 \cos \Lambda'$. The conditions of test can then be associated with an intermediate value of this parameter, which is assumed to be constant along the span of the wing.

TABLE 4A

Evaluation of $\tau = f \,.\, g$

λ	$f(\lambda)$
0	1·25
0·025	0·77
0·05	$0{\cdot}59_5$
0·1	$0{\cdot}40_5$
0·15	0·29
0·2	0·22
0·25	0·18
0·3	0·16
0·35	0·16
0·4	0·17
0·45	$0{\cdot}19_5$
0·5	0·23
0·6	$0{\cdot}32_5$
0·7	$0{\cdot}45_5$
0·8	0·61
0·9	$0{\cdot}79_5$
1·0	1·00

TABLE 4B

$\frac{1}{p}$	$g\left(\frac{1}{p}\right)$
0	0
0·05	0·019
0·1	0·031
0·2	0·051
0·3	0·068
0·4	0·084
0·5	0·100
0·6	0·115
0·7	0·129
0·8	0·142
0·9	0·155
1·0	0·168
1·1	0·181
1·2	0·193
1·3	0·204
1·4	0·216
1·5	0·227

To estimate the aerodynamic coefficients due to deflected controls, consider first a purely two-dimensional ' strip theory '. For wings of uniform taper with a deflected control of spanwise extent $s\eta_1 < y < s\eta_0$,

$$(C_L)_{\text{s.t.}} = \int_{\eta_1}^{\eta_0} a_2\xi \frac{c}{\bar{c}}\, d\eta = \frac{2a_2\xi}{1+\lambda}\int_{\eta_1}^{\eta_0}\{1-(1-\lambda)\eta\}\, d\eta$$

$$(C_l)_{\text{s.t.}} = \int_{\eta_1}^{\eta_0} a_2\xi \frac{c}{\bar{c}}\tfrac{1}{2}\eta\, d\eta = \frac{a_2\xi}{1+\lambda}\int_{\eta_1}^{\eta_0}\{1-(1-\lambda)\eta\}\,\eta\, d\eta\,.$$

As in section 5.1, the factor $(1/\beta)\cos\Lambda'$ from (44) is used as an equivalent two-dimensional allowance for sweepback and compressibility. Thus

$$\left.\begin{aligned}\left[C_L\Big/\Big(\frac{a_2}{a_1}\xi\Big)\right]_{\text{s.t.}} &= \frac{a_1\cos\Lambda'}{\beta(1+\lambda)}\Big[2\eta-(1-\lambda)\eta^2\Big]_{\eta_1}^{\eta_0}\\ \left[C_l\Big/\Big(\frac{a_2}{a_1}\xi\Big)\right]_{\text{s.t.}} &= \frac{a_1\cos\Lambda'}{6\beta(1+\lambda)}\Big[3\eta^2-2(1-\lambda)\eta^3\Big]_{\eta_1}^{\eta_0}\end{aligned}\right\}\quad\ldots\quad\ldots\quad(45)$$

The corresponding values $\{C_L/(a_2/a_1)\xi\}_{\text{l.l.}}$ and $\{C_l/(a_2/a_1)\xi\}_{\text{l.l.}}$ from lifting-line theory may be calculated by means of Ref. 12. Two extreme values of the modified lift slope $(1/\beta)a_1\cos\Lambda'$ are taken; and the calculation outlined in section 5.1 permits interpolation for intermediate lift slopes. The best accuracy is obtained by linear interpolation in the reciprocals, as if $1/C_L$ and $1/C_l$ were linear functions of $\beta/a_1\cos\Lambda'$.

The induced lift and induced rolling moment are given by the differences

$$-\{(C_L)_{\text{s.t.}}-(C_L)_{\text{l.l.}}\}\ \text{and}\ -\{(C_l)_{\text{s.t.}}-(C_l)_{\text{l.l.}}\}\,.$$

In the special case of a uniform incidence with neutral control setting the induced lift so obtained by lifting-line theory requires the practical correction factor

$$\lambda_i = \frac{\frac{1}{\beta}a_1\cos\Lambda' - (a_1)_{\text{eff.}}}{\frac{1}{\beta}a_1\cos\Lambda' - (a_1)_{\text{l.l.}}}\quad\ldots\quad\ldots\quad\ldots\quad\ldots\quad\ldots\quad\ldots\quad(46)$$

$$= 1 + 0{\cdot}032\sqrt{p}\left\{\frac{1+\tau}{\pi}\Big(1+\frac{1+\tau}{\pi}p + 0{\cdot}032p^{3/2}\Big)\right\}^{-1},$$

when the values of $(a_1)_{\text{l.l.}}$ and $(a_1)_{\text{eff.}}$ are substituted from equations (43) and (44). As a practical measure it is sufficient to use $\lambda_i = 1{\cdot}07$. A similar process will estimate the coefficients $(C_L)_{\text{eff.}}$ and $(C_l)_{\text{eff.}}$ due to deflected controls. The principles of lifting-surface theory suggest that the value $(\lambda_i - 1)$ should be reduced as the control chord decreases. The centre of pressure moves further aft and induced effects become smaller. $(\lambda_i - 1)$ is therefore replaced by

$$\mu_i = (\lambda_i - 1)(2 - 4l_2)\,,$$

where l_2 is given in Table 1 (section 4.2). μ_i decreases from about $0{\cdot}07$ to zero as the chord ratio E changes from 1 to 0. Equation (46) may be rewritten as

$$(a_1)_{\text{l.l.}} - (a_1)_{\text{eff.}} = (\lambda_i - 1)\left\{\frac{1}{\beta}a_1\cos\Lambda' - (a_1)_{\text{l.l.}}\right\}.$$

The corresponding equation for the rolling moment from deflected controls is

$$(C_l)_{\text{l.l.}} - (C_l)_{\text{eff.}} = \mu_i\{(C_l)_{\text{s.t.}} - (C_l)_{\text{l.l.}}\}\,.$$

Therefore

$$\left(\frac{\partial C_l}{\partial \xi}\right)_{\text{eff.}} = \frac{a_2}{a_1}\left[\left(\frac{C_l}{\frac{a_2}{a_1}\xi}\right)_{\text{l.l.}} - \mu_i\left\{\left(\frac{C_l}{\frac{a_2}{a_1}\xi}\right)_{\text{s.t.}} - \left(\frac{C_l}{\frac{a_2}{a_1}\xi}\right)_{\text{l.l.}}\right\}\right], \quad \ldots \quad \ldots \quad (47)$$

where $\mu_i = (\lambda_i - 1)(2 - 4l_2)$

and $(C_l)_{\text{s.t.}}$ and $(C_l)_{\text{l.l.}}$ correspond to a low-speed lift slope $a_1 = (a_1)_{\text{test}}$ consistent with (44). If required, $(\partial C_L/\partial \xi)_{\text{eff.}}$ may be estimated similarly.

By equating $(\partial C_l/\partial \xi)_{\text{eff.}}$ and the corrected experimental derivative $(\partial C_l/\partial \xi)_{\text{test}}$, (47) will determine a mean value $(a_2/a_1)_{\text{test}}$ for a particular control surface and Mach number. Ref. 11 shows that, in incompressible flow, a_2/a_1 is a well-defined function of E for any given value of $a_1/(a_1)_T$. It should be verified that consistent values $(a_1)_{\text{test}}$ and $(a_2/a_1)_{\text{test}}$ satisfy the measured quantities. On swept wings with ailerons, however, the thicker boundary layers towards the wing tips may be expected to cause a rather lower value of $(a_2)_{\text{test}}$. $(a_1)_{\text{test}}$ and $(a_2)_{\text{test}}$ are essentially low-speed values and should not vary much with subcritical Mach number. Having related the data from the wind tunnel to these incompressible two-dimensional quantities $(a_1)_{\text{test}}$ and $(a_2)_{\text{test}}$, the corrections to full-scale flight involve the following simple operations:

(*a*) Determine $(a_1)_{\text{flight}}$ from $(a_1)_{\text{test}}$ by means of Fig. 14 of Ref. 11.

(*b*) Use $(a_1)_{\text{flight}}$ to evaluate $\left\{C_l \Big/ \left(\frac{a_2}{a_1}\xi\right)\right\}_{\text{s.t.}}$ from (45).

(*c*) Use $(a_1)_{\text{flight}}$ to determine $\left\{C_l \Big/ \left(\frac{a_2}{a_1}\xi\right)\right\}_{\text{l.l.}}$ whose reciprocal is practically linear between the the two extreme values of $\beta/a_1 \cos \Lambda'$ (section 5.1).

(*d*) Determine $(a_2)_{\text{flight}}$ from $(a_2)_{\text{test}}$ by using Fig. 18 of Ref. 11, which relates a_2 to a_1. If Fig. 18 gives an inconsistent value of $(a_1)_{\text{test}}$, the corresponding $(a_1)_{\text{flight}}$ should be found by repeating operation (*a*) for a fictitious trailing-edge angle and should then be used to evaluate $(a_2)_{\text{flight}}$ from Fig. 18.

(*e*) Evaluate $(\partial C_l/\partial \xi)_{\text{flight}}$ from (47). When the lateral derivative is required from control tests on a half-model, $\left\{C_l \Big/ \left(\frac{a_2}{a_1}\xi\right)\right\}_{\text{l.l.}}$ should be determined in both symmetrical and antisymmetrical cases. To correlate with experiment, the symmetrical value is required in (47). To predict $(\partial C_l/\partial \xi)_{\text{flight}}$, operation (*c*) demands the antisymmetrical $\left\{C_l \Big/ \left(\frac{a_2}{a_1}\xi\right)\right\}_{\text{l.l.}}$.

6. *Effect of Reynolds Number.*—The wind-tunnel results after correction for wall interference require modification before they can be applied to the full-scale conditions. It is mentioned in section 4.6 that the accurate determination of tunnel corrections involves calculations of spanwise loading (section 5.1). These calculations should use values of a_1 corresponding to widely different conditions in the boundary layer. By choosing the mean value of a_1 appropriate to the higher Reynolds numbers of flight, linear interpolation will give the required distribution of lift in flight. Section 5.2 describes a practical procedure, which correlates any corrected experimental derivative $\partial C_l/\partial \xi$ with certain two-dimensional values of a_1 and a_2. When appropriate changes in these values have been estimated from two-dimensional charts, the inverse procedure will predict the required rolling derivative in full-scale flight.

But since corrections will normally be applied by the methods recommended in sections 4.4 and 4.5, these free-stream calculations may be avoided except when the scale effect on rolling power of ailerons is required and when changes of Mach number are to be considered.

Estimations of the two-dimensional coefficients for the wing sections should be made. Reynolds number effects and changes in transition from model experiment to flight are represented by changes in a_1; corresponding changes in a_2, b_1, b_2 (Ref. 11) and m_1, m_2 (Ref. 15) may be deduced satisfactorily from the values of $a_1/(a_1)_T$. The following process expresses scale effect in a form that is equally applicable to two-dimensional and three-dimensional tests.

6.1. *Scale Effect on Incidence Derivatives.*—It will be assumed that the variation of a_1 along the span of a finite wing is not very large, so that a mean value consistent with the tunnel measurements may be used. For incompressible flow the writers recommend the approximate practical formula from section 5.2:

$$\frac{\partial C_L}{\partial \alpha} = (a_1)_{\text{eff.}} = A\left\{\frac{1}{p} + \frac{1+\tau}{\pi} + 0{\cdot}032\sqrt{p}\right\}^{-1}, \quad \ldots \quad \ldots \quad \ldots \quad (44)$$

where

$$p = \frac{1}{A} a_1 \cos \Lambda',$$

$$\tan \Lambda' = \left\{1 - \frac{0{\cdot}8}{A(\lambda+1)}\right\} \tan \Lambda,$$

τ, determined by lifting-line theory, is given approximately by the product of $f(\lambda)$ and $g(1/p)$ in Tables 4A and 4B, and the third term in the bracket represents the effect of induced aerodynamic camber (Ref. 5).

As a consequence of (44), sweepback (Λ) has a considerable influence on the effect of Reynolds number, represented by a change in the two-dimensional a_1. The ratio of the estimated a_1 in flight to its value under the conditions of test is denoted by

$$\alpha_1 = \frac{(a_1)_{\text{flight}}}{(a_1)_{\text{test}}}.$$

Then if $(\partial C_L/\partial \alpha)_{\text{test}}$ is the experimental derivative, corrected for interference, the corresponding full-scale value is

$$\left(\frac{\partial C_L}{\partial \alpha}\right)_{\text{flight}} = \alpha_1 \left(\frac{\partial C_L}{\partial \alpha}\right)_{\text{test}} . \lambda_A , \quad \ldots \quad \ldots \quad \ldots \quad \ldots \quad \ldots \quad \ldots \quad (48)$$

where

$$\lambda_A = \frac{1 + 0{\cdot}3183(1+\tau)p + 0{\cdot}032p^{3/2}}{1 + 0{\cdot}3183(1+\tau)q + 0{\cdot}032q^{3/2}}$$

in which

$$\left.\begin{aligned} p &= \frac{\cos \Lambda'}{A}(a_1)_{\text{test}} \\ q &= \frac{\cos \Lambda'}{A}(a_1)_{\text{flight}} \end{aligned}\right\} . \quad \ldots \quad \ldots \quad \ldots \quad \ldots \quad \ldots \quad \ldots \quad (49)$$

With zero flap setting scale effect changes the distribution of lift in an approximately uniform ratio, so that the same factor $\alpha_1 \lambda_A$ may generally be applied to the rolling moment on one-half of the wing in (40), *i.e.*,

$$\left(\frac{\partial C_l}{\partial \alpha}\right)_{\text{flight}} = \alpha_1 \left(\frac{\partial C_l}{\partial \alpha}\right)_{\text{test}} . \lambda_A . \quad \ldots \quad \ldots \quad \ldots \quad \ldots \quad \ldots \quad \ldots \quad (50)$$

To correct $\partial C_H/\partial \alpha$ for Reynolds number, a mean value of b_1 must be determined at each Reynolds number, since a considerable spanwise variation may be expected. Take

$$\bar{b}_1 = \int_{y_1}^{y_0} b_1 c_f^2 \, dy \Big/ \int_{y_1}^{y_0} c_f^2 \, dy ,$$

where $y_1 < y < y_0$ is the spanwise extent and c_f the chord of the control.

Since

$$\left(\frac{\partial C_m}{\partial \alpha}\right)_{\text{flight}} = -\left(\frac{\partial C_L}{\partial \alpha}\right)_{\text{flight}} \cdot \frac{1 - \frac{4}{3\pi}(1-\lambda)}{\frac{1}{2}(1+\lambda)} \left\{ (l)_{\text{flight}} - \tfrac{1}{4} \right\},$$

it follows that

$$\left(\frac{\partial C_m}{\partial \alpha}\right)_{\text{flight}} = \alpha_1 \lambda_A \left[\frac{(h)_{\text{flight}}}{(h)_{\text{test}}} \left(\frac{\partial C_m}{\partial \alpha}\right)_{\text{test}} + \frac{1 - \frac{4}{3\pi}(1-\lambda)}{2(1+\lambda)} \left(\frac{\partial C_L}{\partial \alpha}\right)_{\text{test}} \left\{ 1 - \frac{(h)_{\text{flight}}}{(h)_{\text{test}}} \right\} \right] \quad (54)$$

where α_1 and λ_A are defined in (48)

and the taper parameter $\lambda = \dfrac{4s}{Ac_0} - 1$

$$= \frac{c_1}{c_0} \text{ for uniformly tapered wings.}$$

6.2. *Scale Effect at Small Lifts.*—Associated with these changes in the incidence derivatives there will be scale effects on the coefficients $C_{H\,0}$, $C_{m\,0}$, defined by

$$\left.\begin{aligned} C_H &= C_{H\,0} + \frac{\partial C_H}{\partial \alpha}(\alpha - \alpha_0) \\ C_m &= C_{m\,0} + \frac{\partial C_m}{\partial \alpha}(\alpha - \alpha_0) \end{aligned}\right\} \quad \ldots \quad (55)$$

Now lift on the wing at zero incidence is attributed to curvature in the centre-line and possibly to asymmetry in the boundary-layer transitions. Lift due to a cambered centre-line may be taken to be proportional to $\partial C_L/\partial \alpha$, so that there should be no pure scale effect on α_0. There may well be, however, discrepancies between wind-tunnel and flight tests due to changes in transition. Although the variation in the derivatives with mean position of transition is understood fairly well, the effect of asymmetry on the two surfaces is very sensitive to trailing-edge shape and cannot be predicted quantitatively. In this field *ad hoc* control testing is indispensable, and the authors wish to emphasize the need for independent changes in the location of transition and its systematic measurement on both wing surfaces (*see* section 3). Systematic experiments of this kind on the model would provide data to show the variations in C_L, C_m and C_H with χ, the distance in terms of the chord between the positions of transition on the upper and lower surfaces (positive when the upper surface transition is forward of the lower). These tests must be done at very low C_L, say at zero incidence, in order to be able to cover a sufficient range of transition movement. Evidence that there is no noticeable scale effect on the variation of the coefficients with the asymmetry of transition is given by Figs. 4 and 5. These figures are taken from the observations on the section 1541a in two-dimensional flow (Ref. 11) made in the R.A.E. No. 2, 11½-ft by 8½-ft Wind Tunnel; the tests were done at three speeds, and within the limits of experimental error the observations lie on straight lines for both C_L and C_H. Figs. 4 and 5 give the values

$$\frac{\partial C_L}{\partial \chi} = 0{\cdot}06\,, \qquad \frac{\partial C_H}{\partial \chi} = -\,0{\cdot}025\,.$$

These values correspond to a trailing-edge angle of about 20 deg. Tests on the 1541 series, in which the trailing-edge angle was varied from 0 deg to 20 deg (Ref. 11), indicate that the values decrease rapidly with decreasing trailing-edge angle. The lift arising from asymmetry of transition acts at $0{\cdot}35c$, whatever the shape of the after half of the section, the front half having been unchanged for the series of aerofoils; this might be a result of general application to all profiles.

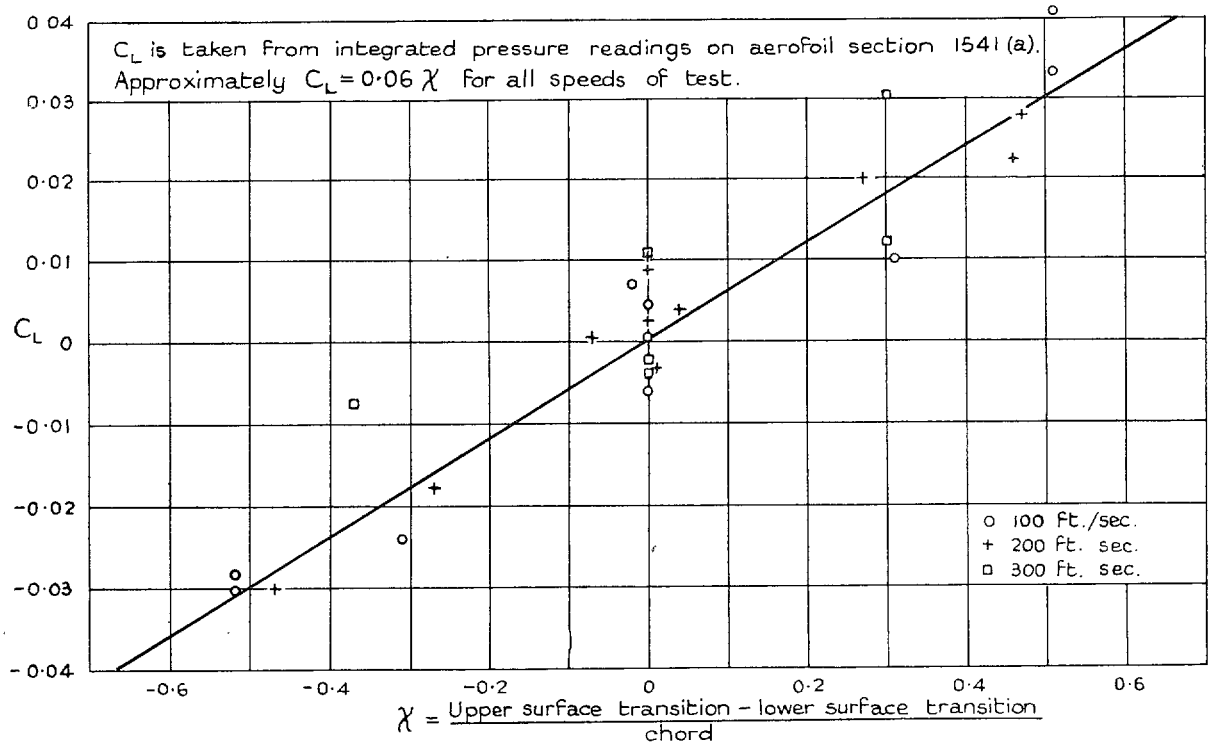

FIG. 4. Scale effect on C_L with variable transition ($\alpha = 0$).

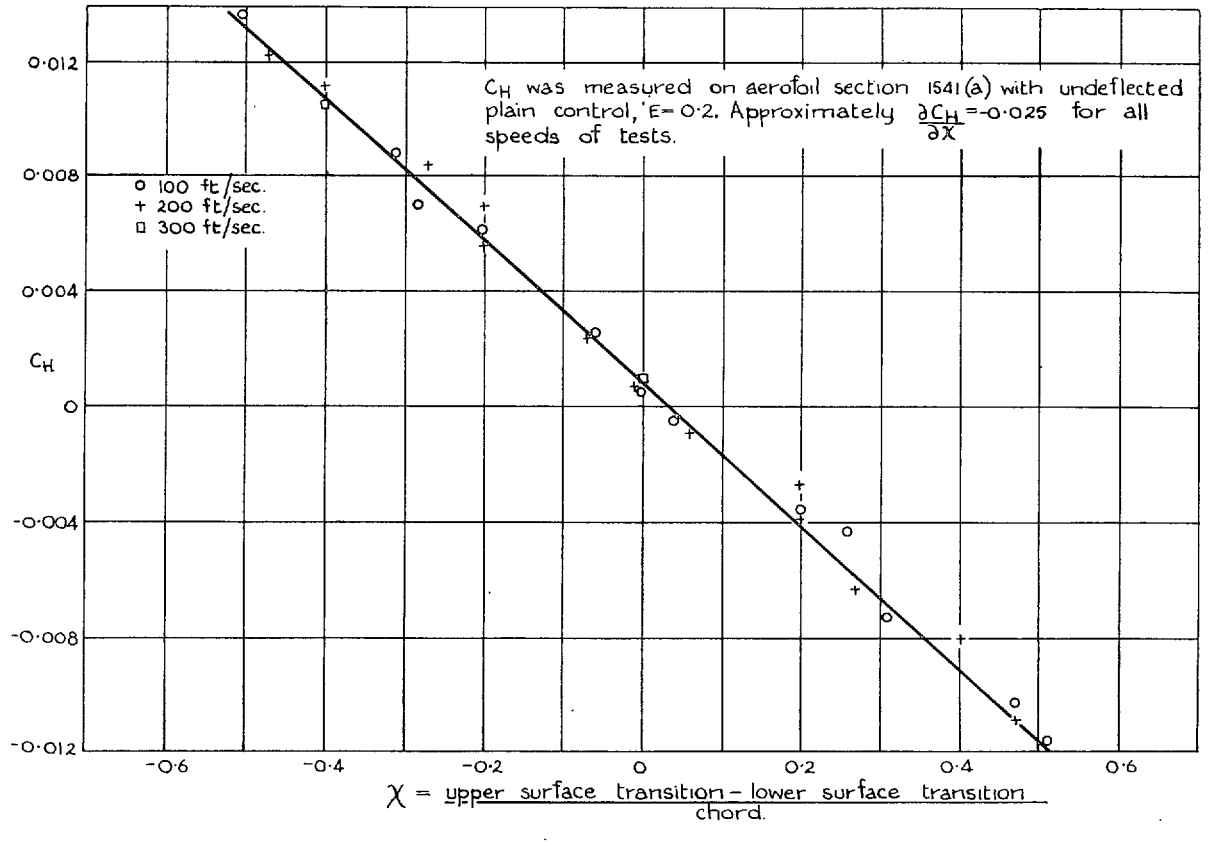

FIG. 5. Scale effect on C_H with variable transition ($\alpha = 0$).

If the recommended experiments are carried out, the change of no-lift angle due to any estimated difference in the extent of the asymmetry in transition, model and full-scale, can be found from the equation

$$(\alpha_0)_{\text{flight}} - (\alpha_0)_{\text{test}} = \frac{\partial C_L/\partial\chi \{(\chi)_{\text{test}} - (\chi)_{\text{flight}}\}}{\partial C_L/\partial\alpha} \quad \ldots \quad (56)$$

The scale effect on the derivative $\partial C_L/\partial\alpha$ is calculated in the way described in section 6.1.

When the model has cambered sections it is necessary to make additional corrections to $C_{H\,0}$ and $C_{m\,0}$, associated with the changes in the two-dimensional derivatives. Since from (15) there is no scale effect on b'/b_1, and aspect ratio effect is unlikely to be important at low lift, it is suggested that the scale effect on $C_{H\,0}$ is the same as for the mean two-dimensional derivative b_1. From (14) there is no scale effect on m'/a_1 and it is suggested that the scale effect on $C_{m\,0}$ is the same as for the two-dimensional derivative a_1. Thus, together with an incremental scale effect due to a change in asymmetry of transition χ,

$$\left.\begin{aligned}(C_{H\,0})_{\text{flight}} &= \beta_1(C_{H\,0})_{\text{test}} + \frac{\partial C_H}{\partial\chi}\{(\chi)_{\text{flight}} - (\chi)_{\text{test}}\} \\ (C_{m\,0})_{\text{flight}} &= \alpha_1(C_{m\,0})_{\text{test}} + \frac{\partial C_m}{\partial\chi}\{(\chi)_{\text{flight}} - (\chi)_{\text{test}}\}\end{aligned}\right\}, \quad \ldots \quad (57)$$

where α_1 and β_1 are defined in (48) and (51), and the derivatives $\partial C_H/\partial\chi$ and $\partial C_m/\partial\chi$ are obtained from special tests.

From (55) the corrections to the experimentally estimated free-stream C_H and C_m at small lift are therefore given by

$$\left.\begin{aligned}(C_H)_{\text{flight}} &= (C_{H\,0})_{\text{flight}} + \beta_1\lambda_B(\partial C_H/\partial\alpha)_{\text{test}}\{\alpha - (\alpha_0)_{\text{flight}}\} \\ (C_m)_{\text{flight}} &= (C_{m\,0})_{\text{flight}} + (\partial C_m/\partial\alpha)_{\text{flight}}\{\alpha - (\alpha_0)_{\text{flight}}\}\end{aligned}\right\}, \quad \ldots \quad (58)$$

where $(\alpha_0)_{\text{flight}}$ is given in (56), $(\partial C_m/\partial\alpha)_{\text{flight}}$ in (54), and $(C_{H\,0})_{\text{flight}}$ and $(C_{m\,0})_{\text{flight}}$ in (57).

6.3. *Scale Effect on Derivatives of Flap Angle.*—The effect of aspect ratio on the derivative $\partial C_H/\partial\xi$ for a three-dimensional model is mainly due to aerodynamic camber, and in the present state of knowledge is somewhat uncertain. The following procedure is therefore suggested for the purpose of corrections to flight conditions.

To account for the spanwise variation in b_2, it is often necessary to evaluate a mean value

$$\bar{b}_2 = \int_{y_1}^{y_0} b_2 c_f^2 \, dy \Big/ \int_{y_1}^{y_0} c_f^2 \, dy$$

and to determine

$$\beta_2 = \frac{\bar{b}_2 \text{ (associated with } (a_1)_{\text{flight}})}{\bar{b}_2 \text{ (associated with } (a_1)_{\text{test}})} \text{ (Ref. 11).}$$

Then it is probably sufficient to take

$$\left(\frac{\partial C_H}{\partial\xi}\right)_{\text{flight}} = \beta_2\left(\frac{\partial C_H}{\partial\xi}\right)_{\text{test}} \cdot \lambda_A, \quad \ldots \quad (59)$$

where λ_A is defined in (48). Indeed the calculations of Ref. 17 for an unswept wing show this to be in remarkable agreement theoretically.

The procedure of section 5.2 may be applied to the derivative $\partial C_L/\partial\xi$, when the necessary calculations by section 5.1 have been carried out. Otherwise the theoretical result, that changes in $\partial C_L/\partial\xi$ and $\partial C_L/\partial\alpha$ with aspect ratio are roughly proportional, indicates the simple scale effect

$$\left(\frac{\partial C_L}{\partial\xi}\right)_{\text{flight}} = \alpha_2\left(\frac{\partial C_L}{\partial\xi}\right)_{\text{test}} \cdot \lambda_A, \quad \ldots \quad (60)$$

where

$$\alpha_2 = \frac{a_2 \text{ (associated with } (a_1)_{\text{flight}})}{a_2 \text{ (associated with } (a_1)_{\text{test}})} \text{ (Ref. 11).}$$

to make a quantitative study beyond an incidence a little below the stall. Any further investigation would require a drastic increase in the Reynolds number of test, unless it were found possible to delay the stall on the model by some experimental control of the boundary layer.

In the absence of complications arising from gaps or from local features which can cause premature separations or breakaway of flow on the model, it seems reasonable to suggest that the considerations of this paper should apply without much modification to the higher incidences of test until turbulent separation at the rear of the aerofoil is marked, say at 4 deg or 5 deg below stalling. The equation (58) will still be valid if the derivatives and α_0 are appropriate to the boundary-layer conditions of transition and rear turbulent separation observed on the model at the given incidence α. The measured no-lift angle, actually giving zero lift in the tunnel, normally corresponds to symmetrical transition points; but $(\alpha_0)_{\text{test}}$ for substitution in (55) may be deduced by using the derivative $\partial C_L/\partial\chi$ (section 6.2), and the value of χ for the incidence α of test. Then the test and flight values of $C_L/(\alpha - \alpha_0)$ can replace $(\partial C_L/\partial\alpha)_{\text{test}}$ and $(\partial C_L/\partial\alpha)_{\text{flight}}$ in (48), which will still apply. The ratio α_1 is not sensitive to mean transition position and can therefore be roughly estimated from the generalised charts (Ref. 11). The presence of turbulent separation, unless very different on the model from the full scale, should not materially affect the ratio α_1. By assuming also that λ_A is not changed appreciably by turbulent separations close to the trailing edge, it follows that (48) will give the required $(\partial C_L/\partial\alpha)_{\text{flight}}$. Hence

$$C_L = (\partial C_L/\partial\alpha)_{\text{flight}}\{\alpha - (\alpha_0)_{\text{flight}}\},$$

where $(\alpha_0)_{\text{flight}}$ is given in (56).

To be consistent with $(\alpha_0)_{\text{test}}$, the test values of C_{H0} and C_{L0} should next be corrected from symmetric to asymmetric transitions as in section 6.2. The test values of $\partial C_H/\partial\alpha$ and $\partial C_m/\partial\alpha$ then follow from (55), and can be corrected to full scale by the procedure of section 6.1. For high incidences $(\alpha_0)_{\text{test}}$ needs no further correction for transition changes between model and full scale, but C_{H0} and C_{m0} may need correction for scale effect on account of camber of the section. The final values of C_m and C_H can then be found for the full-scale Reynolds number from (58).

With the same limitation that separation must not occur far from the trailing edge, the derivatives due to flap setting may be treated as in section 6.3.

In the presence of turbulent separation in any marked degree, there is not as yet any satisfactory procedure for estimating scale effects on hinge and pitching moments. The foregoing discussion is intended to deal with scale effects on smooth-surfaced models representing the basic features of the design. At high incidences in particular it may be argued that the effects of gaps and of nose balance outweigh in importance any likely effect of Reynolds number on the behaviour of the basic unbalanced sealed flaps. Scale effects on the flow through gaps and on the balance of the flaps can only be assessed from systematic researches, from collected data or from experience. If a watch is kept on the model for unusual features of flow, and for positions of boundary-layer transitions and separations, it should be possible to arrive at a reliable opinion regarding the applicability of the model results to full-scale conditions.

7. *Summary of Procedure.*—(i) In the first place it is urged that to obtain useful information on control surfaces from experiments conducted in a wind tunnel, considerable care must be taken both with the construction of the model and with the conditions of test (section 2). Systematic measurements and changes in the locations of boundary-layer transition are strongly advised (section 3). The minimum diameter d of a wire to ensure final transition may be estimated from the formula

$$\frac{V\delta}{\nu} = 5{\cdot}84\sqrt{\left(\frac{Vx}{\nu}\right)}$$

and the accompanying Fig. 1, in which $(Vd/\nu)_{\min}$ is plotted against $V\delta/\nu$ (section 3.1).

(ii) the first correction to be applied to wind-tunnel tests is an increment to the undisturbed wind speed (measured upstream of the model) to take account of the tunnel blockage of the model and its wake (section 4.1).

(iii) Associated with the lift on the model there is a tunnel interference correction to incidence (sections 4.4, 4.5 and 4.6).

(iv) Associated with the lift on the model there is similarly an induced curvature of flow, which together with any residual incidence is expressed as a correction to each required force or moment (sections 4.4, 4.5 and 4.6).

(v) After correction for wall interference the wind-tunnel results are modified to provide estimates of full-scale flight under the conditions of transition predetermined for the tests (section 3). From ratio corrections to the derivatives of the required forces and moments and modifications to their values of zero lift, aerodynamic characteristics of the wing at incidence with and without deflections of the control may be predicted (sections 6.1, 6.2 and 6.3).

7.1. *Collected Formulae for Correcting Two-dimensional Tests.*—

Blockage Correction :

$$\frac{(\Delta V)}{V} = \frac{0{\cdot}62}{\beta^3}\frac{A'}{h^2} + \frac{C_D}{4\beta^2} \cdot \frac{c}{h}$$

Main Correction to Incidence :

$$(\Delta\alpha) = \frac{\pi}{48\beta}\left(\frac{c}{h}\right)^2 \{(C_L)_1(1 - 2l_1) + (C_L)_2(1 - 2l_2)\},$$

where theoretical values of l_2 are given in Table 1.

Main Corrections to Measured Coefficients C_L', C_m', C_H' :

$$(\Delta C_L) = -\frac{\pi a'}{192\beta}\left(\frac{c}{h}\right)^2 C_L',$$

$$(\Delta C_m) = -\frac{\pi m'}{192\beta}\left(\frac{c}{h}\right)^2 C_L',$$

$$(\Delta C_H) = -\frac{\pi b'}{192\beta}\left(\frac{c}{h}\right)^2 C_L',$$

where

$$\frac{a'}{4\pi} = \frac{m'}{-\pi} = \frac{a_1}{(a_1)_T} \cdot \frac{C_L'}{(a_1)'(\alpha' - \alpha_0') + (a_2)'\xi}$$

$$\frac{b'}{b_1} = \left(\frac{b'}{b_1}\right)_T \text{ is given in Table 2.}$$

Scale Effect :

The derivatives $\partial C_L/\partial\alpha$, $\partial C_H/\partial\alpha$, $\partial C_L/\partial\xi$, $\partial C_H/\partial\xi$ are modified by the respective factors α_1, β_1, α_2, β_2, where

$$\alpha_1 = \frac{(a_1)_{\text{flight}}}{(a_1)_{\text{test}}}, \qquad \beta_1 = \frac{(b_1)_{\text{flight}}}{(b_1)_{\text{test}}}, \text{ etc. (Ref. 11).}$$

Derivatives of pitching moment are modified similarly (Ref. 15).

There is probably no scale effect on α_0 other than that arising from changes in transition. For any given positions of boundary-layer transition the coefficients C_{m0}, C_{H0} are modified by the respective factors α_1, β_1, *viz.*,

$$(C_{m0})_{\text{flight}} = \alpha_1(C_{m0})_{\text{test}}, \text{ (about quarter-chord)}$$
$$(C_{H0})_{\text{flight}} = \beta_1(C_{H0})_{\text{test}}.$$

β_1 may vary with α owing to changes in transition. Otherwise the curves of C_H against α would need a constant correction factor for scale effect.

7.2. *Collected Approximate Formulae for Correcting Three-Dimensional Tests in a Closed Tunnel.—Blockage Correction :*

$$\frac{(\Delta V)}{V} = \frac{0{\cdot}62}{\beta^3}\frac{V'}{Ch} + \frac{C_D}{4\beta^2}\frac{S}{C} \text{ (wing)}$$

$$= \frac{0{\cdot}65}{\beta^3}\frac{V'}{Ch} + \frac{C_D}{4\beta^2}\frac{S}{C} \text{ (complete aircraft)}$$

Main Correction to Incidence :

$$(\Delta\alpha)_{3/4} = \frac{4S(C_L)_1}{\pi C}\left[\int_0^1 \frac{\partial}{\partial t}\left\{t\delta_0(y,t)\right\}\sqrt{\left\{1-\left(\frac{t}{s}\right)^2\right\}}\,d\left(\frac{t}{s}\right)\right.$$

$$+\frac{1}{\beta}\int_0^1 \frac{\partial}{\partial t}\left\{t\delta_1(y,t)\right\}\left\{\left(\tfrac{3}{4}-l\right)\frac{c_0}{h}+\frac{y}{h}\tan\Lambda_{3/4}-\frac{t}{h}\tan\Lambda_l\right\}\sqrt{\left\{1-\left(\frac{t}{s}\right)^2\right\}}\,d\left(\frac{t}{s}\right)\Bigg]$$

$$+\frac{4K_0y_0}{CV}\left\{\delta_0(y,y_0)+\frac{\frac{3}{4}c_0+y\tan\Lambda_{3/4}-l_0c_0-y_0\tan\Lambda_0}{\beta h}\,\delta_1(y,y_0)\right\}$$

$$-\frac{4K_1y_1}{CV}\left\{\delta_0(y,y_1)+\frac{\frac{3}{4}c_0+y\tan\Lambda_{3/4}-0{\cdot}3c_0-y_1\tan\Lambda_1}{\beta h}\,\delta_1(y,y_1)\right\}$$

$$+\frac{4K_0\tan\Lambda_0}{CV\beta h}\int_0^{y_0} t\delta_1(y,t)\,dt-\frac{4K_1\tan\Lambda_1}{CV\beta h}\int_0^{y_1} t\delta_1(y,t)\,dt\,,$$

where the parameters $\delta_0(y,t)$, $\delta_1(y,t)$ are defined in (17) (*see* Appendix II) and should be available for any particular tunnel, l is given by (21) and is approximately $l_1 \doteq \frac{1}{4}$,

$$K_0y_0 - K_1y_1 = \tfrac{1}{4}VS(C_L)_2$$

$$K_0y_0^2 - K_1y_1^2 = sVS(C_l)_2\,\{\text{contribution to } C_l' \text{ due to } \xi\}:$$

$\tan\Lambda_{3/4}$, $\tan\Lambda_0$, $\tan\Lambda_1$ are obtained from

$$\tan\Lambda_l = \tan\Lambda - \frac{c_0}{s}(1-\lambda)(l-\tfrac{1}{4})$$

by substituting $l = \frac{3}{4}$, l_0 (equation (27)), $0{\cdot}3$ respectively.

$(\Delta\alpha)_{3/4}$ varies (with y) along the span and a process of averaging gives the correction to be applied to the measured incidence

$$(\Delta\alpha) = 0{\cdot}6 \text{ (elliptic mean)} + 0{\cdot}4 \text{ (chord mean)}$$

$$= \int_0^1 (\Delta\alpha)_{3/4}\left\{\frac{2{\cdot}4}{\pi}\sqrt{\left[1-\left(\frac{y}{s}\right)^2\right]}+0{\cdot}8\frac{cs}{S}\right\}d\left(\frac{y}{s}\right).$$

Without flaps,

$$(\Delta\alpha) = \frac{SC_L'}{C}\,\delta\,,$$

where δ is given in Fig. 2 (square tunnel) and Fig. 3 (duplex tunnel), in which the abscissa $(\sigma + 1{\cdot}5/A)$ may be generalised as $[\sigma + (3/A\beta)(\frac{3}{4}-l)]$.

Residual Corrections to Measured Coefficients.—These correspond to the removal of a residual local incidence $(\Delta\alpha)_{3/4} - (\Delta\alpha)$ and a local camber

$$(\Delta\gamma) = \frac{S(C_L)_1}{2\pi C} \cdot \frac{c}{\beta\bar{h}} \int_0^1 \frac{\partial}{\partial t}\{t\delta_1(y,t)\} \Big/ \left[1 - \left(\frac{t}{s}\right)^2\right] d\left(\frac{t}{s}\right) + \frac{K_0 y_0}{2CV} \cdot \frac{c}{\beta\bar{h}}\,\delta_1(y,y_0) - \frac{K_1 y_1}{2CV} \cdot \frac{c}{\beta\bar{h}}\,\delta_1(y,y_1)\,,$$

which varies (with y) along the span.

$$(\Delta C_L) = 0\,,$$

$$(\Delta C_l) = -\frac{\partial C_l}{\partial\alpha} \int_0^s \{(\Delta\alpha)_{3/4} - \Delta\alpha\}\, cy\sqrt{(s^2 - y^2)}\, dy \Big/ \int_0^s cy\sqrt{(s^2 - y^2)}\, dy\,,$$

$$(\Delta C_m) = -A \tan\Lambda\, (\Delta C_l) - m' \cos\Lambda \int_0^s \left(\frac{c}{\bar{c}}\right)^2 (\Delta\gamma)\, \frac{dy}{s}\,,$$

$$(\Delta C_H) = -\frac{\partial C_H}{\partial\alpha} \int_{y_1}^{y_0} \left\{(\Delta\alpha)_{3/4} - (\Delta\alpha) - 2(\Delta\gamma) + \frac{b'}{b_1}(\Delta\gamma)\right\} c_f^{\,2}\sqrt{(s^2 - y^2)}\, dy \Big/ \int_{y_1}^{y_0} c_f^{\,2}\sqrt{(s^2 - y^2)}\, dy\,,$$

where b'/b_1 is given in Table 2.

Scale Effect:

$$\left(\frac{\partial C_L}{\partial\alpha}\right)_{\text{flight}} = \alpha_1 \left(\frac{\partial C_L}{\partial\alpha}\right)_{\text{test}} \cdot \lambda_A$$

$$\left(\frac{\partial C_l}{\partial\alpha}\right)_{\text{flight}} = \alpha_1 \left(\frac{\partial C_l}{\partial\alpha}\right)_{\text{test}} \cdot \lambda_A$$

$$\left(\frac{\partial C_H}{\partial\alpha}\right)_{\text{flight}} = \beta_1 \left(\frac{\partial C_H}{\partial\alpha}\right)_{\text{test}} \cdot \lambda_B$$

$$\left(\frac{\partial C_m}{\partial\alpha}\right)_{\text{flight}} = \alpha_1\lambda_A \left[\frac{(h)_{\text{flight}}}{(h)_{\text{test}}} \left(\frac{\partial C_m}{\partial\alpha}\right)_{\text{test}} + \frac{1 - \frac{4}{3\pi}(1 - \lambda)}{2(1 + \lambda)} \left(\frac{\partial C_L}{\partial\alpha}\right)_{\text{test}} \left\{1 - \frac{(h)_{\text{flight}}}{(h)_{\text{test}}}\right\}\right]$$

where

$$\left.\begin{aligned} \lambda_A &= \frac{1 + 0{\cdot}3183(1 + \tau)p + 0{\cdot}032p^{3/2}}{1 + 0{\cdot}3183(1 + \tau)q + 0{\cdot}032q^{3/2}} \\ \lambda_B &= \frac{1 + 0{\cdot}3183(1 + \tau)p + 0{\cdot}016\frac{b'}{b_1}p^{3/2}}{1 + 0{\cdot}3183(1 + \tau)q + 0{\cdot}016\frac{b'}{b_1}q^{3/2}} \end{aligned}\right\}$$

with

$$p = \frac{\cos\Lambda'}{A}(a_1)_{\text{test}}\,, \quad q = \frac{\cos\Lambda'}{A}(a_1)_{\text{flight}}\,,$$

$$\tan\Lambda' = \left\{1 - \frac{0\ 8}{A(\lambda + 1)}\right\} \tan\Lambda\,.$$

C_m is the coefficient of pitching moment about the mean elliptic quarter-chord axis.

h is determined from Ref. 15, Fig. 65 for the appropriate values of $a_1/(a_1)_T$.

At small lifts,

$$(C_H)_{\text{flight}} = \frac{\partial C_H}{\partial \chi}\left\{(\chi)_{\text{flight}} - (\chi)_{\text{test}}\right\} + \beta_1\left[(C_{H\,0})_{\text{test}} + \lambda_B\left(\frac{\partial C_H}{\partial \alpha}\right)_{\text{test}}\left\{\alpha - (\alpha_0)_{\text{flight}}\right\}\right]$$

$$(C_m)_{\text{flight}} = \frac{\partial C_m}{\partial \chi}\left\{(\chi)_{\text{flight}} - (\chi)_{\text{test}}\right\} + \alpha_1(C_{m\,0})_{\text{test}} + \left(\frac{\partial C_m}{\partial \alpha}\right)_{\text{flight}}\left\{\alpha - (\alpha_0)_{\text{flight}}\right\},$$

where

$$(\alpha_0)_{\text{flight}} = (\alpha_0)_{\text{test}} + \frac{\partial C_L/\partial \chi}{\partial C_L/\partial \alpha}\left\{(\chi)_{\text{test}} - (\chi)_{\text{flight}}\right\}.$$

With deflected flaps the aerodynamic coefficients are split into contributions due to α and ξ. The latter contributions are corrected as follows :

$$\left(\frac{\partial C_L}{\partial \xi}\right)_{\text{flight}} = \alpha_2\left(\frac{\partial C_L}{\partial \xi}\right)_{\text{test}} \cdot \lambda_A$$

$$\left(\frac{\partial C_H}{\partial \xi}\right)_{\text{flight}} = \beta_2\left(\frac{\partial C_H}{\partial \xi}\right)_{\text{test}} \cdot \lambda_A$$

$$\left(\frac{\partial C_m}{\partial \xi}\right)_{\text{flight}} = \alpha_2\lambda_A\left[\frac{\frac{1}{4} - (m_2/\alpha_2)_{\text{flight}}}{\frac{1}{4} - (m_2/a_2)_{\text{test}}}\left(\frac{\partial C_m}{\partial \xi}\right)_{\text{test}}\right.$$

$$\left. + \frac{1 - \frac{4}{3\pi}(1-\lambda)}{2(1+\lambda)}\left(\frac{\partial C_L}{\partial \xi}\right)_{\text{test}}\frac{(m_2/a_2)_{\text{flight}} - (m_2/a_2)_{\text{test}}}{\frac{1}{4} - (m_2/a_2)_{\text{test}}}\right].$$

where m_2 may be estimated from Ref. 15, Figs. 65 and 67, for the appropriate values of $a_1/(a_1)_T$ (interpolating or extrapolating for the required value of E). It should be noted that, in the notation of Ref. 15,

$$\frac{m_2}{a_2} = \frac{m_1}{a_1} - \frac{m}{a_2} = (\tfrac{1}{4} - h) - \frac{m}{a_2}.$$

$(\partial C_l/\partial \xi)_{\text{test}}$ requires two corrections, firstly from the symmetrical loading on the half-model to the practical condition of antisymmetrical ailerons at the Reynolds number of test, and secondly a scale effect. $(\partial C_l/\partial \xi)_{\text{flight}}$ should be estimated from a special computation by the procedure of section 5.2, which includes the effect of compressibility.

8. NOTATION

A	Aspect ratio
A'	Cross-sectional area of wing
a_1, $(a_1)'$	Free-stream, measured, two-dimensional $\partial C_L/\partial\alpha$
a_2, $(a_2)'$	Free-stream, measured, two-dimensional $\partial C_L/\partial\xi$
a'	Free-stream two-dimensional $\partial C_L/\partial\gamma$
b	Breadth of tunnel (along span of model)
b_1, $\bar{b}_1$	Two-dimensional $\partial C_H/\partial\alpha$, spanwise average
b_2, $\bar{b}_2$	Two-dimensional $\partial C_H/\partial\xi$, spanwise average
b'	Two-dimensional $\partial C_H/\partial\gamma$
C	Cross-sectional area of working-section of tunnel
C_D	*Profile drag force/$(\frac{1}{2}\rho V^2 S)$
C_H, C_H'	Free-stream, measured, hinge moment/$(\frac{1}{2}\rho V^2 S_f \bar{c}_f)$
C_L, C_L'	*Free-stream, measured, $L/(\frac{1}{2}\rho V^2 S)$
C_l, C_l'	*Free-stream, measured, $\mathscr{L}/(\frac{1}{2}\rho V^2 S \,.\, 2s)$
C_m, C_m'	*Free-stream, measured, $\mathscr{M}(\frac{1}{2}\rho V^2 S\bar{c})$
C_{H0}, C_{m0}	Values of C_H, C_m at zero lift
$(C_L)_1$, $(C_L)_2$	Contributions to C_L' due to α, ξ
c	Chord of wing, measured in direction of wind
c_0, c_1	Value of c at root, tip of wing
$\bar{c}$	Mean chord $(= S/2s)$
c_f	Chord of flap measured downstream from hinge
$\bar{c}_f$	Mean chord of flap $S_f/(y_0 - y_1)$
d	Diameter of transition wire
E	Flap chord ratio (c_f/c)
eff.	Suffix denoting value for the three-dimensional wing
f, g	Parameters defined in equation (44)
h	Height of tunnel (at right-angles to span of model)
$(h)_{\text{flight}}$, $(h)_{\text{test}}$	Corresponding two-dimensional aerodynamic centres (Ref. 15, Fig. 65)
K, K_0, K_1	Strengths of horse-shoe vortices (section 4.5)
L	Aerodynamic lift force

---

* If measurements are made on a half-wing, the coefficients C_D, C_L', C_l', C_m' should of course be determined by replacing S by $\frac{1}{2}S$, *e.g.*,

$$C_l' = \frac{\text{Measured } \mathscr{L} \text{ on the half-wing}}{\frac{1}{2}\rho V^2 . \frac{1}{2} S . 2s},$$

where $\frac{1}{2}S$ is the surface area of the half-wing.

$\mathscr{L}$	Aerodynamic rolling moment
l	Centre of pressure of wing section (fraction of chord from leading edge)
l_0	Value of l defined in section 4.5, equation (27)
l_1, l_2	l due to α, ξ (l_2 given in Table 1)
l.l.	Suffix denoting lifting-line theory
M	Mach number
$\mathscr{M}$	Aerodynamic pitching moment (about axis through mean elliptic quarter-chord point, unless otherwise stated)
m_1, m_2, m'	Two-dimensional $\partial C_m/\partial\alpha$, $\partial C_m/\partial\xi$, $\partial C_m/\partial\gamma$
m	Parameter occurring in lifting-line theory—usually $m = 15$
p, q	Values of $a_1 \cos \Lambda'/\beta A$ corresponding to test, flight conditions
R	Reynolds number (Vc/ν)
S	Surface area of wing
S_f	Surface area of flap (or aileron)
s	Semi-span of wing or span of half-model
s.t.	Suffix denoting two-dimensional strip theory
T	Suffix denoting theoretical value
t	Thickness of wing (section 4.1)
t	Spanwise co-ordinate measured from wing root denoting semi-span of horse-shoe vortex
V	Undisturbed velocity of free stream
V'	Volume occupied by model
w	Upward component of velocity induced by tunnel interference
x	Chordwise distance (from leading edge of root section)
$\bar{x}$	Value of x at centre of pressure of half-wing
x_0	Local position of lifting-line corresponding to equation (19)
x	Distance of transition wire from leading edge (section 3.1)
y	Distance from wing root measured along span
$y_1 < y < y_0$	Spanwise extent of aileron
$\bar{y}$	Value of y at centre of pressure of half-wing
α	Incidence of wing in free stream
α'	Measured incidence of wing
α_0, α_0'	Free-stream, measured, value of α at zero lift
α_1, α_2	$(a_1)_{\text{flight}}/(a_1)_{\text{test}}$, $(a_2)_{\text{flight}}/(a_2)_{\text{test}}$
$(\Delta\alpha)_{3/4}$	Local incidence at three-quarter chord due to tunnel interference
β	$\sqrt{(1 - M^2)}$, compressibility factor

NOTATION—*continued*

$\beta_1,\ \beta_2$	$(\bar{b}_1)_{\text{flight}}/(\bar{b}_1)_{\text{test}},\ (\bar{b}_2)_{\text{flight}}/(\bar{b}_2)_{\text{test}}$
Γ	Circulation round wing
γ	Camber defined in Ref. 2, equation (13.01)
Δ	Prefix denoting increment to a quantity due to tunnel interference
δ	Thickness of boundary layer (section 3.1)
δ	Interference parameter (equation (24))
$\delta_0(y,t),\ \delta_1(y,t)$	Parameters representing w at y due to K of semi-span t (equation (17))
$\eta,\ \eta_0,\ \eta_1$	$y/s,\ y_0/s,\ y_1/s$: spanwise parameters
θ	Parameter of chordwise distance $(= \cos^{-1}(1 - 2x/c))$
$\theta_1,\ \theta_2$	Value of θ at hinge-line, nose of flap
Λ	Angle of sweepback of quarter-chord line
Λ'	Equivalent angle of sweepback (equation (44))
$\Lambda_l\ (\Lambda_0,\ \Lambda_1,\ \Lambda_{3/4})$	Angle of sweepback at l-chord $(l = l_0,\ 0{\cdot}3,\ \frac{3}{4})$
λ	c_1/c_0 or $(4s/Ac_0 - 1)$, taper parameter
λ	Nose balance as fraction of flap chord (section 4.2)
$\lambda_A,\ \lambda_B$	Parameters used in correction for Reynolds number (section 6.1)
$\lambda_i,\ \mu_i$	Parameters used in computing lift and rolling moment (section 5.2)
ν	Kinematic viscosity
ν	Suffix used in lifting-line theory (section 5.1)
ξ	Angle of deflection of flap
ρ	Density of fluid
σ	s/b
τ	Parameter in approximate formula (43)
ϕ	Spanwise parameter (defined by $y = s\cos\phi$)
χ	$[x$(upper surface transition) $- x$(lower surface transition)$]/c$

9. *Calculated Examples.*—In conclusion a number of examples have been worked out in order to illustrate the orders of magnitude of corrections due to tunnel interference and due to scale effect.

From the approximate formulae, given in section 7.2, the interference in a square tunnel has been evaluated for two particular plan-forms over a range of spans. The examples include :

(*a*) complete models placed symmetrically,

(*b*) half models with aileron mounted on one wall.

In case (*b*) the scale effect has also been estimated under certain conditions.

The calculations have been carried out for wings 4 and 6 (Ref. 27, Fig. 3) of uniform taper, defined by

$$A = 4; \quad \lambda = \tfrac{1}{2}; \quad \tan \Lambda = 0 \text{ and } \tfrac{2}{3} \text{ respectively,}$$

with an outboard half-span aileron of constant chord ratio, $E = 0{\cdot}2$.

The basic sectional data in Table 5A have been determined from Refs. 11, 15, and 26 for a conventional aerofoil with

$$t/c = 0{\cdot}10; \quad \text{trailing-edge angle} = 10 \text{ deg.}$$

The assumed values

$$\frac{(a_1)_{\text{test}}}{(a_1)_T} = 0{\cdot}78 \; ; \qquad \frac{(a_1)_{\text{flight}}}{(a_1)_T} = 0{\cdot}90$$

correspond to a change of Reynolds number from approximately

$$(R)_{\text{test}} = 2 \times 10^6 \text{ to } (R)_{\text{flight}} = 5 \times 10^7 .$$

Rough values for the derivatives of test, corrected to free-stream conditions, have been estimated from the two-dimensional data by considering approximate lifting-surface theory (Table 5B). The following have been used in the evaluation of wind-tunnel interference:

Corrected derivative	*Wing* 4 $\Lambda = 0$ deg	*Wing* 6 $\Lambda \simeq 34$ deg
$\partial C_L/\partial\alpha$	3·57	$3{\cdot}23_5$
$\partial C_l/\partial\alpha$	0·757	$0{\cdot}686_5$
$\partial C_H/\partial\alpha$	−0·204	−0·187
$\partial C_L/\partial\xi$	0·628	0·569

It has been further assumed that

$$\bar{y} = \frac{\mathscr{L}}{L} = \frac{2s\,\partial C_l/\partial\xi}{\partial C_L/\partial\xi} = 0{\cdot}62s \, .$$

The quantities $(\Delta\alpha)$, (ΔC_l), (ΔC_m) and (ΔC_H) have been computed directly from section 7.2 for various sizes of wing

$$\sigma = s/b = 0{\cdot}2, \; 0{\cdot}3, \; 0{\cdot}4,$$

using the values of $\delta_0(y,t)$, $\delta_1(y,t)$ from Ref. 27.

Curves of

$$\frac{(\Delta\alpha)}{C_L'} \text{ and } \frac{(\Delta C_m)}{C_L'} \text{ against } \sigma$$

are shown in Fig. 6 for cases (*a*) and (*b*), in which the wing is at incidence but the aileron undeflected. It should be noted that $(\Delta C_m)/C_L'$ is negligible for $\sigma < 0{\cdot}25$, but may increase rapidly with σ, so that a correction of the order $0{\cdot}005\bar{c}$ to the aerodynamic centre is likely to occur, when $\sigma = 0{\cdot}35$.

Acum (Ref. 27) has shown that although the distribution of $(\Delta\alpha)_{3/4}$, is greatly influenced by sweep, its mean value $(\Delta\alpha)$ is practically independent of sweep for both square and duplex tunnels, when an elliptic distribution of lift is assumed (Ref. 27, Figs. 4 and 5). After the correction $(\Delta\alpha)$ has been applied to the incidence of test, the residual corrections (ΔC_m), (ΔC_l) and (ΔC_H) to the measured coefficients of pitching, rolling and hinge moments, defined in section 7.2, are dependent on :

(i) the spanwise distribution of $\{(\Delta\alpha)_{3/4} - (\Delta\alpha)\}$

(ii) the distribution of induced camber $(\Delta\gamma)$.

For a given spanwise distribution of lift, it is supposed that the chordwise variation of induced upwash is linear. It follows that $\Delta\gamma$ is independent of sweep, although it has a marked effect on $\{(\Delta\alpha)_{3/4} - (\Delta\alpha)\}$. Since by the definition of $(\Delta\alpha)$ there is no appreciable residual correction (ΔC_L), (ΔC_m) is virtually independent of pitching axis, but nevertheless can vary a good deal with sweep. (ΔC_l) is determined entirely by (i) and though usually not large may change its sign for different angles of sweep. (ΔC_H) on the other hand is largely influenced by (ii) since the camber derivative b' is large compared with b_1 ; the effect of sweep is therefore less marked in this case.

The values of $(\Delta\alpha)/C_L'$ and $(\Delta C_m)/C_L'$ have been compared in Fig. 6. For a given C_L', $(\Delta\alpha)$ is practically the same for both wings, but for the complete wings in the square tunnel there is some increase in (ΔC_m) with sweep.

The interference on corresponding half-wings fitted with outboard half-span ailerons of constant chord ratio $E = 0{\cdot}2$ in a square tunnel has also been computed. The growth of $(\Delta\alpha)$, (ΔC_m), (ΔC_l) and (ΔC_H) with model size is shown in Fig. 7, where the influence of change of sweep is seen by comparing the dotted and full curves. The measured lift coefficient is split into two contributions

$$C_L' = (C_L)_1 + (C_L)_2 ,$$

which correspond to a uniform incidence α and to an aileron deflection ξ respectively. The tunnel interference due to $(C_L)_1$ is precisely that in Fig. 6 for a duplex tunnel and that due to $(C_L)_2$ is considered separately.

The values are shown plotted against σ in Fig. 7. It is found that, apart from the main correction $(\Delta\alpha)$ to incidence, the residual corrections to the aerodynamic coefficients are negligible for $\sigma < 0{\cdot}25$. The rapid numerical increase in these corrections for larger values of σ is very considerable. Some of the formulae of section 7.2 are then unreliable; and it is emphasised that wind-tunnel staff should be prepared to carry out calculations of wall interference by the methods of section 4.6 when $\sigma > 0{\cdot}35$.

For a model of span $\sigma = 0{\cdot}35$, the following values are obtained :—

Interference correction	*Wing* 4 $\Lambda = 0$ deg	*Wing* 6 $\Lambda \simeq 34$ deg
$(\Delta\alpha)$ per radian α	0·114	0·104
(ΔC_m) per radian α	0·020	0·018
(ΔC_l) per radian α	0·005	−0·001
(ΔC_H) per radian α	0·0055	0·008
$(\Delta\alpha)$ per radian ξ	0·0156	0·0123
(ΔC_m) per radian ξ	0·0035	0·0046
(ΔC_l) per radian ξ	−0·0002	−0·0008
(ΔC_H) per radian ξ	0·0017	0·0019

It is concluded that the corrections due to $(C_L)_2$ are often determined reasonably well by neglecting sweepback. But when $\partial C_L/\partial\xi$ is large the variation in $(\Delta\alpha)/(C_L)_2$ with sweep may become appreciable. For large models at incidence the corrections $(\Delta\alpha)/\alpha$, $(\Delta C_m)/\alpha$, $(\Delta C_l)/\alpha$ and $(\Delta C_H)/\alpha$ may all be important and should always include the effect of induced camber. For all practical purposes $(\Delta\alpha)/\alpha$ is decreased by sweep in the ratio of the lift slopes $\partial C_L/\partial\alpha$.

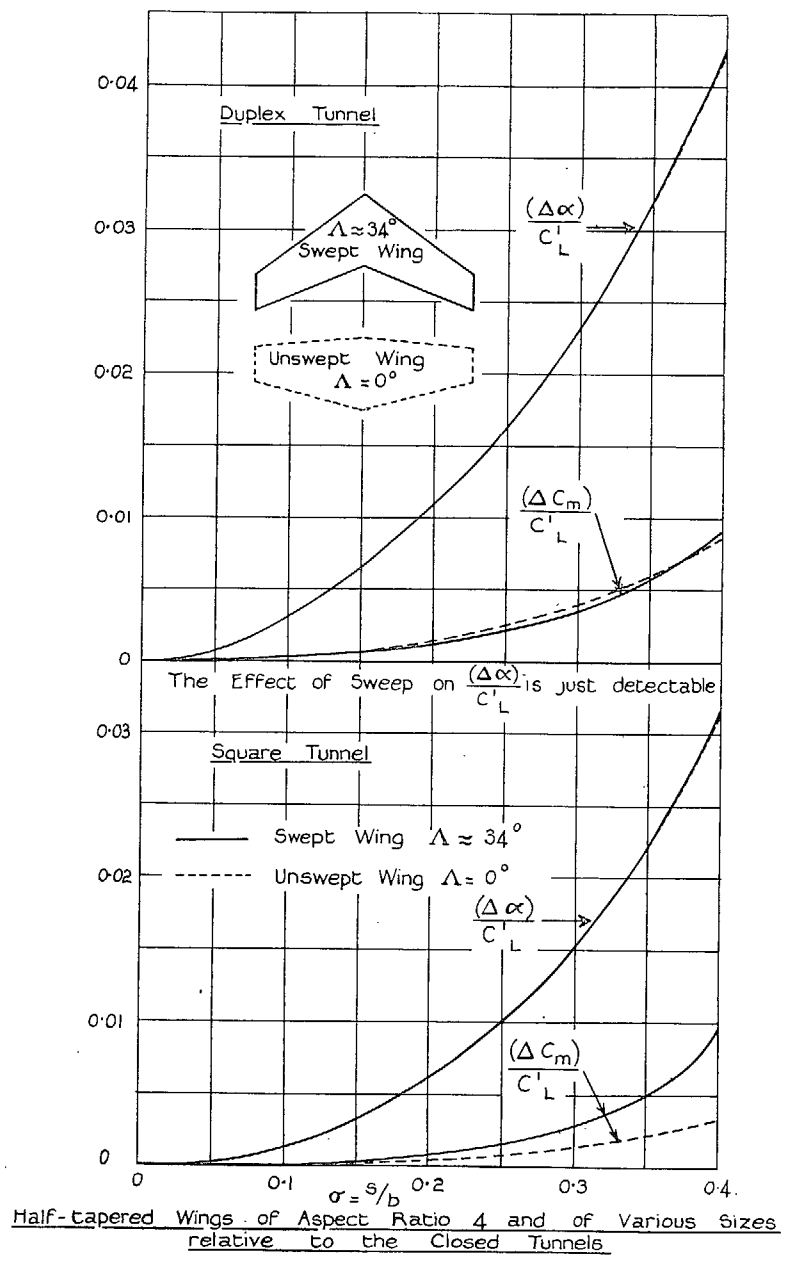

FIG. 6. Calculated tunnel interference.
Swept and unswept wings at uniform incidence.

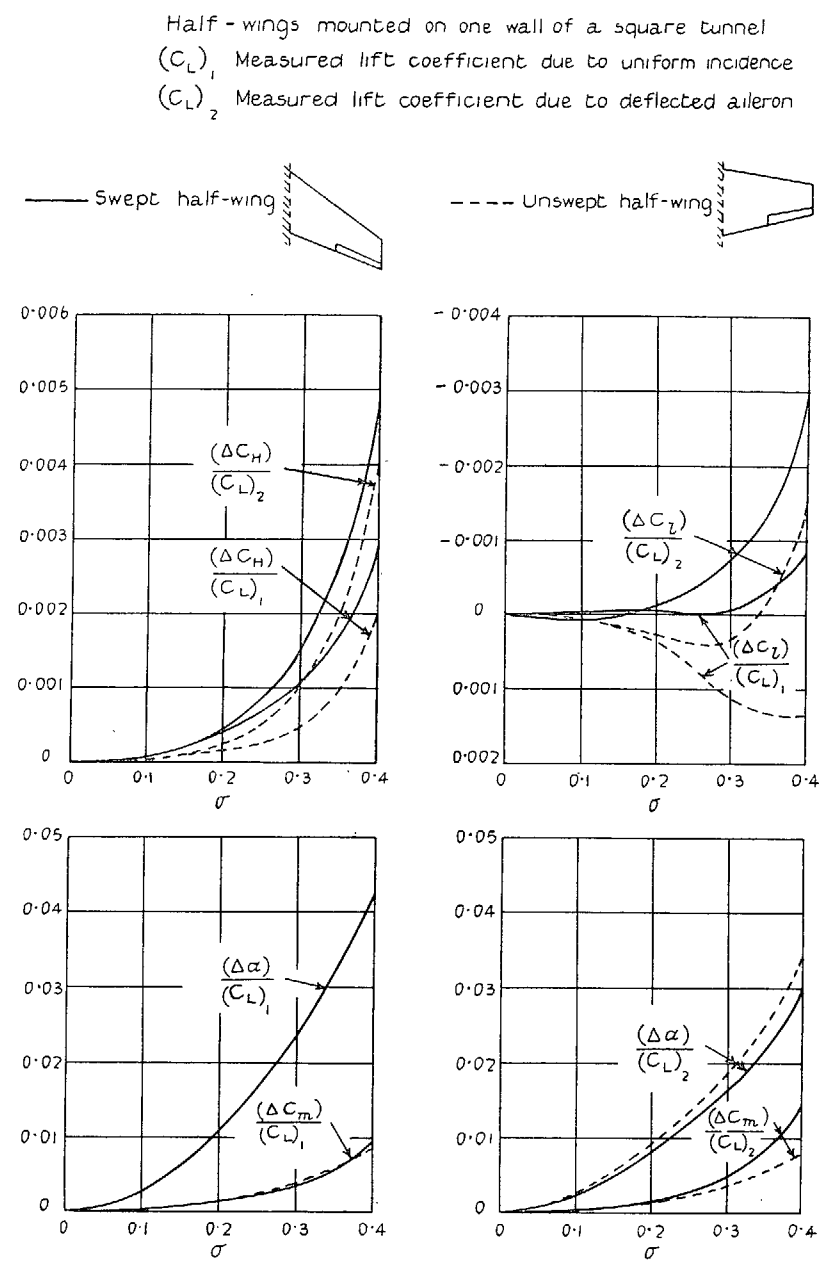

FIG. 7. Calculated tunnel interference.
Swept and unswept half-wings with ailerons.

Calculated Corrections to Derivatives

TABLE 5A

Derivative	Test $R = 2 \times 10^6$	Flight $R = 5 \times 10^7$	Ratio
$a_1/(a_1)_T$	0·78	0·90	
a_1	5·293	6·107	$\alpha_1 = 1 \cdot 154$
a_2	2·392	3·163	$\alpha_2 = 1 \cdot 322$
b_1	−0·328	−0·333	$\beta_1 = 1 \cdot 016$
b_2	−0·597	−0·733	$\beta_2 = 1 \cdot 228$
h	0·237	0·251	1·060
$\frac{1}{4} - m_2/a_2$	0·441	0·453	1·027

TABLE 5B

$\sigma = 0 \cdot 35$

Derivative	Measured $R = 2 \times 10^6$	Test $R = 2 \times 10^6$	Flight $R = 5 \times 10^7$	Tunnel interference	Scale effect
$\partial C_L/\partial\alpha$	3·608	3·235	3·567	−0·373	+0·332
$\partial C_t/\partial\alpha$	0·767	0·686	0·757	−0·081	+0·071
$\partial C_H/\partial\alpha$	−0·215	−0·187	−0·179	+0·028	+0·008
$\partial C_m/\partial\alpha$	0·031	0·046	−0·003	+0·015	−0·049
$\partial C_L/\partial\xi$	0·612	0·569	0·719	−0·043	+0·150
$\partial C_H/\partial\xi$	−0·344	−0·340	−0·399	+0·004	−0·059
$\partial C_m/\partial\xi$	−0·253	−0·249	−0·327	+0·004	−0·078

For the purpose of illustrating the magnitudes of tunnel interference and scale effect on the various aerodynamic derivatives the swept half-wing with aileron (Ref. 27, Wing 6) has been taken. The size of model $\sigma = 0{\cdot}35$ has been selected for Table 5B, where on the basis of the given free-stream derivatives of test the corresponding hypothetical measured values (with corrections for tunnel blockage but no further interference) have been obtained :

e.g.,

$$\frac{\partial C_m'}{\partial \alpha'} = \left(\frac{\partial C_m}{\partial \alpha}\right)_{\text{test}} \left\{1 + \frac{(\Delta\alpha)}{\alpha'}\right\} - \frac{(\Delta C_m)}{(C_L)_1} \frac{\partial C_L'}{\partial \alpha'}$$

where

$$\frac{(\Delta\alpha)}{\alpha'} = 0{\cdot}1155;$$

$$\frac{\partial C_m'}{\partial \xi} = \left(\frac{\partial C_m}{\partial \xi}\right)_{\text{test}} + \frac{(\Delta\alpha)}{\xi}\left(\frac{\partial C_m}{\partial \alpha}\right)_{\text{test}} - \frac{(\Delta C_m)}{(C_L)_2} \frac{\partial C_L'}{\partial \xi}$$

where

$$\frac{(\Delta\alpha)}{\xi} = 0{\cdot}0132\,.$$

In Table 5B, also, the scale effects corresponding to the two-dimensional data have been calculated in accordance with section 7.2. The derivative $\partial C_l/\partial \xi$ has not been estimated, as the large correction from symmetrical loading to the practical condition of antisymmetrical ailerons requires a special calculation (section 5.2).

In practice the changes in the derivatives due to tunnel interference and scale effect should not normally exceed the values illustrated in Table 5B, except in the case of scale effect on hinge moments, where, because a trailing-edge angle of 10 deg has been assumed, there is little variation in b_1 and b_2 with change in a_1 (Ref. 11, Figs. 29 and 31).

Tunnel interference is never likely to be large for the derivative $\partial C_H/\partial \xi$.

Apart from $\partial C_m/\partial \alpha$ the largest percentage correction due to interference will often occur for $\partial C_H/\partial \alpha$.

Scale effect on $\partial C_L/\partial \xi$ (and $\partial C_l/\partial \xi$) will often be large and scale effect in the case of hinge moments will become very important, when the trailing-edge angle is much different from 10 deg.

It is stressed that, in deducing control derivatives from tests, corrections for scale effect may be more important than corrections for tunnel interference. As a routine both corrections should be applied by wind-tunnel staff.

REFERENCES

No.	*Author*	*Title, etc.*
1	A. D. Young and H. B. Squire ..	Blockage corrections in a closed rectangular tunnel. R. & M. 1984. June, 1945.
2	H. Glauert	Wind tunnel interference on wings, bodies and airscrews. R. & M. 1566. 1933.
3	J. S. Thompson	Present methods of applying blockage corrections in a closed rectangular high speed wind tunnel. R.A.E. Report Aero. 2225. A.R.C. 11,385. January, 1948. (Unpublished.)
4	H. M. Lyon	An approximate method of calculating the effect of the interference of a closed tunnel on hinge moments of control surfaces. Aero. Departmental Note Wind Tunnels 567. A.R.C. 5803. May, 1942. (Unpublished.)

REFERENCES—*continued*

No.	*Author*	*Title, etc.,*
5	H. C. Garner	Note on aerodynamic camber. R. & M. 2820. April, 1950.
6	E. N. Jacobs, K. E. Ward and R. M. Pinkerton.	The characteristics of 78 related airfoil sections from tests in the variable-density wind tunnel. N.A.C.A. Report 460. 1933.
7	H. Glauert and A. S. Hartshorn ..	The interference of wind channel walls on the downwash angle and the tail-setting to trim. R. & M. 947. 1924.
8	H. C. Garner	Note on interference in a wind tunnel of octagonal section. A.R.C. 6659. June, 1943. (Unpublished.)
9	H. C. Garner	Note on the interference on a part-wing mounted symmetrically on one wall of a wind tunnel of octagonal section. C.P.5. March, 1947.
10	H. C. Garner	An approximate theoretical determination of the pressure distribution on a finite wing with control flaps in steady motion. A.R.C. 9554. April, 1946. (Unpublished.)
11	L. W. Bryant, A. S. Halliday and A. S. Batson.	Two-dimensional control characteristics. R. & M. 2730. Parts I, II and III. April, 1950.
12	H. Multhopp	The calculation of the lift distribution of aerofoils. *L.F.F.*, Vol. 15, No. 4, 1938. R.T.P. Translation No. 2392. (A.R.C. 8516.)
13	J. H. Preston, N. E. Sweeting and Miss D. K. Cox.	The experimental determination of the two-dimensional interference on a large chord Piercy 12/40 aerofoil in a closed tunnel fitted with a flexible roof and floor. R. & M. 2007. September, 1944.
14	F. N. Kirk	Wind tunnel tests on tunnel corrections to hinge moments of control surfaces. R.A.E. Tech. Note Aero. 1277 (W.T.). A.R.C. 7148. 1943. (Unpublished.)
15	L. W. Bryant, A. S. Halliday and A. S. Batson.	Two-dimensional control characteristics. Part IV. Variation of pitching moments with incidence and control angle. R. & M. 2730. April, 1950.
16	H. H. B. M. Thomas and M. Lofts..	Application of thin aerofoil theory to controls having set-back hinge balance, with analysis of wind tunnel data on aerofoils of finite thickness. R. & M. 2256. July, 1945.
17	H. C. Garner and A. S. Halliday ..	An investigation of a part-wing test on an aileron and methods of computing aileron characteristics. A.R.C. 8922. August, 1945. (Unpublished.)
18	S. Goldstein and A. D. Young ..	The linear perturbation theory of compressible flow, with applications to wind-tunnel interference. R. & M. 1909. July, 1943.
19	H. Glauert	*The Elements of Aerofoil and Airscrew Theory.* Cambridge University Press. 1926.
20	J. H. Preston, N. E. Sweeting and F. H. Burstall.	Experiments on the measurement of transition position by chemical methods. R. & M. 2014. March, 1945.
21	E. J. Richards and F. H. Burstall..	The ' china-clay ' method of indicating transition. R. & M. 2126. August, 1945.
22	W. E. Gray	A simple visual method of recording boundary layer transition (liquid film). R.A.E. Tech. Note Aero. 1816. A.R.C. 10,028. August, 1946. (Unpublished.)
23	L. W. Bryant and A. S. Batson ..	Experiments on the effect of transition on control characteristics, with a note on the use of transition wires. R. & M. 2164. November, 1944.
24	A. Fage	The smallest size of a spanwise surface corrugation which affects boundary-layer transition on an aerofoil. R. & M. 2120. January, 1943.
25	B. J. Eisenstadt	Boundary-induced upwash for yawed and swept-back wings in closed circular wind tunnels. N.A.C.A. Tech. Note 1265. May, 1947.
26	H. C. Garner	Simple evaluation of the theoretical lift slope and aerodynamic centre of symmetrical aerofoils. R. & M. 2847. October, 1951.
27	W. E. A. Acum	Corrections for symmetrical swept and tapered wings in rectangular wind tunnels. R. & M. 2777. April, 1950.
28	F. W. J. Olver	Transformation of certain series occurring in aerodynamic interference theory. *Quart. J. Mech. App. Math.*, Vol. II, Part 4. 1949.
29	W. S. Brown	Wind tunnel corrections on ground effect. R. & M. 1865. 1938.

APPENDIX I

Validity of Elliptic Loading in Section 4.4

Further calculations are given to test the validity of assuming an elliptic spanwise loading when determining the tunnel interference on wings at a uniform incidence or with a deflected full-span control.

At the outset of section 4.4, it has been assumed that an elliptic distribution of lift may be used to determine the tunnel interference on a complete wing inclined to the undisturbed stream or a symmetrical tail model with a deflected full-span elevator. This assumption was partly based on the evidence given by Glauert in Ref. 2, Fig. 10, where it is shown that uniform loading

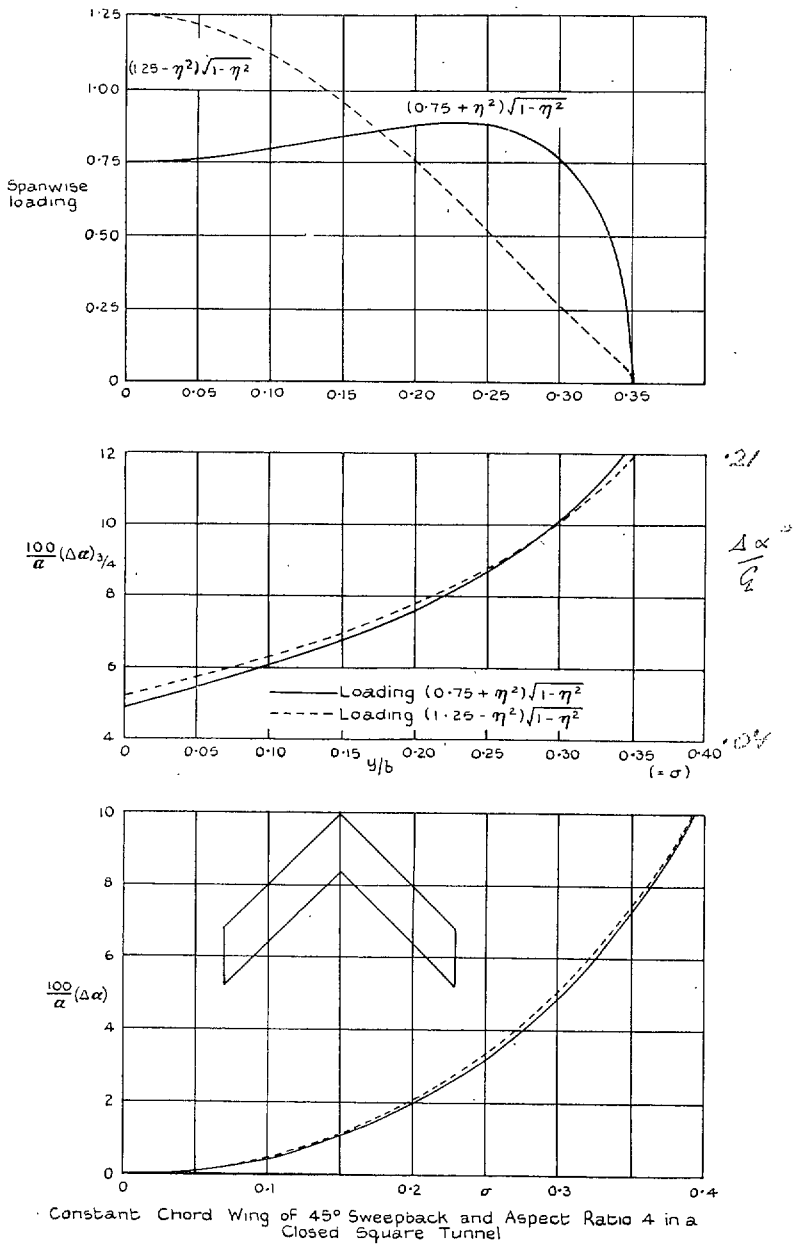

FIG. 8. Calculated tunnel interference. Effect of varying the spanwise loading on wings of different size.

may be taken if only 10 per cent accuracy is required. This evidence suggests that calculations for a square tunnel are likely to reveal any serious deficiencies in the assumption. The interference has therefore been computed by the method of Ref. 27 (Acum, 1950) for constant-chord wings

of 45-deg sweepback, and aspect ratio 4 placed symmetrically in a closed tunnel of square section. The following extreme spanwise loadings have been taken:

$$(0{\cdot}75 + \eta^2)\sqrt{(1 - \eta^2)} \text{ and } (1{\cdot}25 - \eta^2)\sqrt{(1 - \eta^2)},$$

where $-1 \leqslant \eta = y/s \leqslant 1$ denotes the wing span.

In Fig. 8 the interference correction to incidence as a percentage of the incidence of test $100(\Delta\alpha)/\alpha$ has been plotted against

$$\sigma = \frac{\text{wing semi-span}}{\text{tunnel breadth}},$$

using a measured lift slope $\partial C_L/\partial\alpha = 3{\cdot}25$. In the special case $\sigma = 0{\cdot}35$ the local percentage tunnel-induced upwash angle at the three-quarter chord locus of the wing

$$\frac{100}{\alpha}(\Delta\alpha)_{3/4}$$

has been plotted against y/b. The effect of the extreme variation in spanwise loading is shown to be trivial in each case. The variation in $(\Delta\alpha)/\alpha$ with spanwise loading for a given measured C_L' never exceeds $\pm 0{\cdot}1$ per cent and the maximum variation in the local $(\Delta\alpha)_{3/4}/\alpha$ is only $\pm 0{\cdot}2$ per cent, when $\sigma = 0{\cdot}35$. It is concluded that for the purpose of computing tunnel interference (section 4.4), it is accurate enough to assume an elliptic spanwise loading.

APPENDIX II

Methods of Computing δ_0 and δ_1

The quantities δ_0 and δ_1 are defined in section 4.4 by equation (17). Given a tunnel of height h and sectional area C, the wall interference is equivalent to sets of images of a single horse-shoe vortex of strength K, of span $-t < y < t$ and with bound vortex position $x = x_0$. At a distance y from the centre of the tunnel the images produce an upwash angle $\varepsilon_0(y,t) + \varepsilon_1(y,t)$, which is represented by the two parameters

$$\left.\begin{aligned} \delta_0(y,t) &= \frac{CV}{4Kt}\varepsilon_0(y,t) \\ \delta_1(y,t) &= \frac{CV}{4Kt}\frac{h}{x - x_0}\varepsilon_1(y,t) \end{aligned}\right\}.$$

For most purposes $\delta_1(y,t)$ is taken to be independent of x, so that the upwash angle varies linearly along each wing chord. It is usual to place a wing in the centre plane of the tunnel (midway between the roof and floor in the case of a horizontal stream), but it may be necessary to consider a wing above or below the centre plane. This problem has been examined by Brown[29] (1938) for rectangular tunnels.

Rectangular Tunnels.—Imagine a uniformly loaded horizontal model of span $2t$ placed symmetrically in the plane $z = 0$ at a distance d above the floor of the tunnel of breadth b and height h. Then from Ref. 29, page 3, due to tunnel interference the upwash angle at the bound vortex or centre of pressure is

$$\varepsilon_0(y,t) = -\frac{K}{4\pi V}\left[\left(\sum_{-\infty}^{\infty}\sum\right)'\left\{\frac{bm-y+t}{(bm-y+t)^2+4h^2n^2}-\frac{bm-y-t}{(bm-y-t)^2+4h^2n^2}\right\}\right.$$
$$\left.-\left(\sum_{m=-\infty}^{\infty}\sum_{n=-\infty}^{\infty}\right)\left\{\frac{bm-y+t}{(bm-y+t)^2+4(hn-d)^2}-\frac{bm-y-t}{(bm-y-t)^2+4(hn-d)^2}\right\}\right],$$

where $\left(\sum_{-\infty}^{\infty}\sum\right)'$ indicates that (m,n) takes all possible pairs of integral values except (0,0). Then

$$\varepsilon_0(y,t) = +\frac{K}{4\pi Vb}\left[\Omega\left(\frac{t+y}{b}\right)+\Omega\left(\frac{t-y}{b}\right)\right],$$

where

$$\Omega(\sigma) = \left(\sum_{-\infty}^{\infty}\sum\right)\frac{m-\sigma}{(m-\sigma)^2+\left(\frac{2h}{b}\right)^2n^2}-\sum_{m=-\infty}^{\infty}\sum_{n=-\infty}^{\infty}\frac{m-\sigma}{(m-\sigma)^2+\left(\frac{2h}{b}\right)^2\left(n-\frac{d}{h}\right)^2}$$
$$=\frac{1}{\sigma}+\frac{\pi b}{2h}\sum_{m=-\infty}^{\infty}\left\{\coth\frac{\pi b(m-\sigma)}{2h}-\frac{\sinh\frac{\pi b(m-\sigma)}{h}}{\cosh\frac{\pi b(m-\sigma)}{h}-\cos\frac{2\pi d}{h}}\right\}.$$

When the model is in the centre plane and $d = \frac{1}{2}h$,

$$\Omega(\sigma) = \frac{1}{\sigma}+\frac{\pi b}{h}\sum_{m=-\infty}^{\infty}\operatorname{cosech}\frac{\pi b}{h}(m-\sigma).$$

Hence

$$\delta_0(y,t) = \frac{h}{16\pi t}\left\{\Omega\left(\frac{t+y}{b}\right)+\Omega\left(\frac{t-y}{b}\right)\right\}.$$

For a small wing, it follows that

$$\delta_0 = \delta_0(0,0) = \frac{h}{8\pi b}\left(\frac{d\Omega}{d\sigma}\right)_{\sigma=0}.$$

$$\frac{d\Omega}{d\sigma} = -\frac{1}{\sigma^2}+\frac{\pi^2b^2}{4h^2}\left[\operatorname{cosech}^2\frac{\pi b\sigma}{2h}+\frac{2\left\{1-\cosh\frac{\pi b\sigma}{h}\cos\frac{2\pi d}{h}\right\}}{\left\{\cosh\frac{\pi b\sigma}{h}-\cos\frac{2\pi d}{h}\right\}^2}\right]$$
$$+\frac{\pi^2b^2}{2h^2}\sum_{m=1}^{\infty}\left[\operatorname{cosech}^2\frac{\pi b(m-\sigma)}{2h}+\frac{2\left\{1-\cosh\frac{\pi b(m-\sigma)}{h}\cos\frac{2\pi d}{h}\right\}}{\left\{\cosh\frac{\pi b(m-\sigma)}{h}-\cos\frac{2\pi d}{h}\right\}^2}\right]$$

Therefore, in the limiting case as $\sigma \to 0$,

$$\frac{d\Omega}{d\sigma} \to \frac{\pi^2 b^2}{4h^2}\left[-\frac{1}{3}+\frac{2}{1-\cos\dfrac{2\pi d}{h}}\right]$$
$$+\frac{\pi^2 b^2}{2h^2}\sum_{m=1}^{\infty}\left[\operatorname{cosech}^2\frac{\pi bm}{2h}+\frac{2\left\{1-\cosh\dfrac{\pi bm}{h}\cos\dfrac{2\pi d}{h}\right\}}{\left\{\cosh\dfrac{\pi bm}{h}-\cos\dfrac{2\pi d}{h}\right\}^2}\right].$$

Thus

$$\delta_0 = \delta_0(0,0) = \frac{\pi b}{16h}\left[-\frac{1}{6}+\frac{1}{1-\cos\dfrac{2\pi d}{h}}\right.$$
$$\left.+\sum_{m=1}^{\infty}\left\{\operatorname{cosech}^2\frac{\pi bm}{2h}+\frac{2\left(1-\cosh\dfrac{\pi bm}{h}\cos\dfrac{2\pi d}{h}\right)}{\left(\cosh\dfrac{\pi bm}{h}-\cos\dfrac{2\pi d}{h}\right)^2}\right\}\right].$$

Therefore, for a small model in the centre plane, where $d = \frac{1}{2}h$,

$$\delta_0 = \frac{\pi b}{4h}\left[\frac{1}{12}+\sum_{m=1}^{\infty}\coth\frac{\pi bm}{h}\operatorname{cosech}\frac{\pi bm}{h}\right],$$

which is evaluated in Table 3.

The chordwise increment in the upwash angle from the rectangular tunnel walls is determined from Ref. 29, page 9, whence

$$\varepsilon_1(y,t) = \frac{K(x-x_0)}{4\pi V}\left[\left\{\frac{1}{(x-x_0)^2+4d^2}+\frac{1}{(y+t)^2+4d^2}\right\}\frac{y+t}{\{(x-x_0)^2+(y+t)^2+4d^2\}^{1/2}}\right.$$
$$-\left\{\frac{1}{(x-x_0)^2+4d^2}+\frac{1}{(y-t)^2+4d^2}\right\}\frac{y-t}{\{(x-x_0)^2+(y-t)^2+4d^2\}^{1/2}}$$
$$\left.+\left(\sum_{-\infty}^{\infty}\right)'\{G_n(y-bm+t)-G_n(y-bm-t)\}\right],$$

where
$$G_n(y) = \left\{\frac{1}{(x-x_0)^2+4(hn-d)^2}+\frac{1}{y^2+4(hn-d)^2}\right\}\frac{y}{\{(x-x_0)^2+y^2+4(hn-d)^2\}^{1/2}}$$
$$-\left\{\frac{1}{(x-x_0)^2+4h^2n^2}+\frac{1}{y^2+4h^2n^2}\right\}\frac{y}{\{(x-x_0)^2+y^2+4h^2n^2\}^{1/2}}.$$

It is advisable to determine the upwash correction at the tail of a complete model of an aeroplane from this exact form for $\varepsilon_1(y,t)$. But as far as the interference on a single wing is concerned, $\varepsilon_1(y,t)$ may be expanded in odd powers of $(x-x_0)$ and terms of the order $(x-x_0)^3$ may be neglected. This is equivalent to an assumption that the chordwise upwash gradient is constant, and gives

$$\delta_1(y,t) = \frac{bh^2}{16\pi t}\left[\tfrac{1}{2}\sum_{m=1}^{\infty}\left\{\frac{1}{(bm+y-t)^2}+\frac{1}{(bm-y-t)^2}-\frac{1}{(bm+y+t)^2}-\frac{1}{(bm-y+t)^2}\right\}\right.$$
$$+\sum_{n=-\infty}^{\infty}\sum_{m=-\infty}^{\infty}\left\{H_{2(n-d/h)}(y-bm+t)-H_{2(n-d/h)}(y-bm-t)\right\}$$
$$\left.-2\sum_{n=1}^{\infty}\sum_{m=-\infty}^{\infty}\left\{H_{2n}(y-bm+t)-H_{2n}(y-bm-t)\right\}\right],$$

where for $n \geqslant 1$, $H_n(y) = \dfrac{y(y^2+2h^2n^2)}{h^2n^2(y^2+h^2n^2)^{3/2}}$.

The infinite double series may be evaluated by Brown's[29] process, in which the residue of terms in the double summation for which either $|m| > M$ or $|n| > N$ is calculated by the simple approximations

$$\sum_{n=-N}^{N}\sum_{m=-\infty}^{-(M+1)}\left[H_{2(n-d/h)}(y-bm+t)-H_{2(n-d/h)}(y-bm-t)\right]$$
$$=\frac{2t}{b}\sum_{n=-N}^{N}\sum_{m=-\infty}^{-(M+1)}\left[H_{2(n-d/h)}(y-bm+\tfrac{1}{2}b)-H_{2(n-d/h)}(y-bm-\tfrac{1}{2}b)\right]$$
$$=\frac{2t}{b}\sum_{n=-N}^{N}\left[\frac{1}{4(hn-d)^2}-H_{2(n-d/h)}(y+bM+\tfrac{1}{2}b)\right];$$

and

$$\sum_{n=-\infty}^{-(N+1)}\sum_{m=-\infty}^{\infty}\left[H_{2(n-d/h)}(y-bm+t)-H_{2(n-d/h)}(y-bm-t)\right]$$
$$=\frac{2t}{b}\sum_{n=-\infty}^{-(N+1)}\frac{1}{2(hn-d)^2}.$$

Hence

$$\sum_{n=-\infty}^{\infty}\sum_{m=-\infty}^{\infty}\left[H_{2(n-d/h)}(y-bm+t)-H_{2(n-d/h)}(y-bm-t)\right]$$
$$=\sum_{n=-N}^{N}\sum_{m=-M}^{M}\left[H_{2(n-d/h)}(y-bm+t)-H_{2(n-d/h)}(y-bm-t)\right]$$
$$+\frac{2t}{b}\sum_{n=-N}^{N}\left[-H_{2(n-d/h)}(y+bM+\tfrac{1}{2}b)+H_{2(n-d/h)}(y-bM-\tfrac{1}{2}b)\right]$$
$$+\frac{2t}{b}\sum_{n=-\infty}^{\infty}\frac{1}{2(hn-d)^2},$$

where

$$\sum_{n=-\infty}^{\infty}\frac{1}{2(hn-d)^2}=\frac{\pi^2\operatorname{cosec}^2(\pi d/h)}{2h^2}.$$

The four infinite series in the first bracket of $\delta_1(y,t)$ are Trigamma functions*,

$$\Psi'\left(1+\frac{y}{b}\right)=b^2\sum_{m=1}^{\infty}\frac{1}{(bm+y)^2}.$$

Then $\delta_1(y,t)$ may be evaluated from the formula

$$\delta_1(y,t)=\frac{h^2}{32\pi bt}\left\{\Psi'\left(1+\frac{y-t}{b}\right)+\Psi'\left(1-\frac{y+t}{b}\right)-\Psi'\left(1+\frac{y+t}{b}\right)-\Psi'\left(1-\frac{y-t}{b}\right)\right\}$$
$$+\frac{bh^2}{16\pi t}\left[\sum_{n=-N}^{N}\sum_{m=-M}^{M}\left\{H_{2(n-d/h)}(y-bm+t)-H_{2(n-d/h)}(y-bm-t)\right\}\right.$$
$$\left.-2\sum_{n=1}^{N}\sum_{m=-M}^{M}H_{2n}(y-bm+t)-H_{2n}(y-bm-t)\right\}\Bigg]$$
$$+\frac{h^2}{8\pi}\Bigg[-\sum_{n=-N}^{N}\left\{H_{2(n-d/h)}\left(y+bM+\tfrac{1}{2}b\right)-H_{2(n-d/h)}\left(y-bM-\tfrac{1}{2}b\right)\right\}.$$
$$+2\sum_{n=1}^{N}\left\{H_{2n}\left(y+bM+\tfrac{1}{2}b\right)-H_{2n}\left(y-bM-\tfrac{1}{2}b\right)\right\}$$
$$+\frac{\pi^2}{2h^2}\operatorname{cosec}^2\frac{\pi d}{h}-\frac{\pi^2}{6h^2}\Bigg].$$

* Tabulated values of the Trigamma function Ψ' will be found in *Tables of the Higher Mathematical Functions*, Volume II by H. T. Davis. The Principal Press Inc., Indiana, U.S.A. 1935.

In the usual case, when the model is in the centre plane, $d = \frac{1}{2}h$ and this reduces to the simpler expression

$$\delta_1(y,t) = \frac{h^2}{32\pi bt}\left\{\Psi'\left(1+\frac{y-t}{b}\right)+\Psi'\left(1-\frac{y+t}{b}\right)-\Psi'\left(1+\frac{y+t}{b}\right)-\Psi'\left(1-\frac{y-t}{b}\right)\right\}$$
$$-\frac{bh^2}{8\pi t}\sum_{n=1}^{N}\sum_{m=-M}^{M}(-1)^n\{H_n(y-bm+t)-H_n(y-bm-t)\}$$
$$+\frac{\pi}{24}+\frac{h^2}{4\pi}\sum_{n=1}^{N}(-1)^n\left\{H_n\left(y+bM+\tfrac{1}{2}b\right)-H_n\left(y-bM-\tfrac{1}{2}b\right)\right\}.$$

In practice M and N may be taken as small integers, $M = 2$, $N = 2$ say, and $\delta_1(y,t)$ is easily evaluated from the approximate formula

$$\delta_1(y,t) = \frac{h^2}{32\pi bt}\left\{\Psi'\left(1+\frac{y-t}{b}\right)+\Psi'\left(1-\frac{y+t}{b}\right)-\Psi'\left(1+\frac{y+t}{b}\right)-\Psi'\left(1-\frac{y-t}{b}\right)\right\}$$
$$-\frac{bh^2}{8\pi t}\sum_{n=1}^{N}\sum_{m=-M}^{M}(-1)^n\{H_n(y-bm+t)-H_n(y-bm-t)\}+R_{MN},$$

where the small remainder is virtually independent of y and may be calculated as

$$R_{MN} = \frac{\pi}{24}+\frac{1}{2\pi}\sum_{n=1}^{N}(-1)^n\frac{b(2M+1)\{b^2(2M+1)^2+8h^2n^2\}}{n^2\{b^2(2M+1)^2+4h^2n^2\}^{3/2}}.$$

For a small wing it follows that

$$\delta_1(0,0) = \frac{h^2b}{16\pi t}2t\frac{\partial}{\partial t}\left[-\sum_{m=1}^{\infty}\frac{1}{(bm+t)^2}-2\sum_{n=1}^{\infty}\sum_{m=-\infty}^{\infty}(-1)^nH_n(bm+t)\right]_{t=0}.$$

Now $$\frac{\partial H_n}{\partial y} = \frac{2h^2n^2-y^2}{(y^2+h^2n^2)^{5/2}}.$$

Hence

$$\delta_1(0,0) = \frac{h^2}{4\pi b^2}\left[\sum_{m=1}^{\infty}\frac{1}{m^3}-\sum_{n=1}^{\infty}\sum_{m=-\infty}^{\infty}(-1)^n\frac{2b^3h^2n^2-b^5m^2}{(b^2m^2+h^2n^2)^{5/2}}\right],$$

where $\sum_1^{\infty} 1/m^3 = 1{\cdot}2020569$. Values of $\delta_1(0,0)$ for a small wing placed symmetrically in a rectangular tunnel are given in Table 3 of section 4.4.

A more precise method of evaluating $\delta_1(y,t)$, when the model is in the centre plane, is to transform the double series

$$\sum_{n=1}^{\infty}\sum_{m=-\infty}^{\infty}(-1)^n\{H_n(y-bm+t)-H_n(y-bm-t)\}$$

into a more rapidly convergent series of modified Bessel functions[28] (Olver, 1949). In this form $\delta_1(y,t)$ is easily computable to any given accuracy. This method is preferable to the foregoing procedure, which has, however, been used satisfactorily.

Values of $\delta_0(y,t)$ and $\delta_1(y,t)$ for rectangular tunnels ($b/h = 1$, 9/7, 2, 18/7) are tabulated in Ref. 27 (Acum, 1950).

Circular Tunnels.—For a uniformly loaded wing of span $2t$ symmetrically placed along a diameter of a tunnel of circular section of radius a, it follows at once from Ref. 2, p. 13, that

$$\varepsilon_0(y,t) = \frac{a^2 tK}{2\pi V(a^4 - t^2y^2)}.$$

Hence

$$\delta_0(y,t) = \frac{a^4}{8(a^4 - t^2y^2)}.$$

There is no corresponding expression for $\delta_1(y,t)$. But Eisenstadt[25] (1947) has produced an exact theory and tabulated values of

$$\frac{4\pi a^2}{Kt}\, w(y,t)$$

for a circular tunnel with a horse-shoe vortex of strength K and span $0 < y < t$. Hence

$$\delta_0(y,t) + \frac{x - x_0}{2a}\,\delta_1(y,t) = \frac{1}{16}\,\frac{4\pi a^2}{Kt}\left\{w(y,t) + w(-y,t)\right\}.$$

Eisenstadt includes swept bound vortices with -45 deg $< \Lambda < 45$ deg and gives $w(y,t)$ for several values of $(x - x_0)$. By definition $\delta_1(y,t)$ corresponds to an unswept bound vortex and is determined by the limiting condition as $x \to x_0$. Numerical values of δ_0 and δ_1 are given in the following tables :

TABLE 6

Values of $\delta_0(y,t)$ and $\delta_1(y,t)$ for a Circular Tunnel

y/a	$\delta_0(y,t)$ for $t/a =$				
	0	0·25	0·45	0·70	0·90
0	0·1250	0·1250	0·1250	0·1250	0·1250
0·2	0·1250	0·1253	0·1260	0·1275	0·1292
0·5	0·1250	0·1270	0·1317	0·1425	0·1567
0·7	0·1250	0·1289	0·1388	0·1645	0·2073
0·9	0·1250	0·1317	0·1495	0·2073	0·3635

y/a	$\delta_1(y,t)$ for $t/a =$				
	0	0·25	0·45	0·70	0·90
0	0·2500	0·250	0·251	0·254	0·258
0·2	0·250	0·253	0·258	0·264	$0·27_5$
0·5	0·263	0·269	0·290	0·33	0·40
0·7	0·278	0·290	$0·32_5$	0·44	0·65
0·9	0·301	$0·32_5$	0·40	0·67	1·7

For a wing of sheared elliptical plan-form there is a simplification in the approximate method of interference correction, when an elliptic distribution of lift may be assumed (section 4.4). For this purpose it will be supposed that $\delta_1(y,t)$ is proportional to $\delta_0(y,t)$ the ratio being determined from Table 6.

From equations (20) and (24) of section 4.4

$$(\Delta\alpha) = \frac{SC_L'}{C}\delta = \frac{4}{\pi}\int_0^1 (\Delta\alpha)_{3/4}\sqrt{\{1-(y/s)^2\}}\, d(y/s),$$

where

$$(\Delta\alpha)_{3/4} = \frac{4SC_L'}{\pi C}\int_0^1 \left(1 + \frac{x-x_0}{2a}\cdot\frac{\delta_1}{\delta_0}\right)\frac{\partial}{\partial t}\left\{t\delta_0(y,t)\right\}\sqrt{\{1-(t/s)^2\}}\, d(t/s)\,,$$

where $x(y)$ and $x_0(t)$ denote values of x at $\frac{3}{4}c$ and lc respectively. Fig. 6 shows that δ is not sensitive to angle of sweep, and this is chosen so that the locus of the lifting line $x_0(t)$ is unswept and x_0 is independent of t. Then

$$(x - x_0) = c(\tfrac{3}{4} - l) = c_0(\tfrac{3}{4} - l)\sqrt{\{1-(y/s)^2\}}\,.$$

On writing $y = s\cos\phi$, $t = s\cos\psi$,

$$\begin{aligned}(\Delta\alpha)_{3/4} &= -\frac{4SC_L'}{\pi C}\left\{1 + \frac{\delta_1}{\delta_0}\frac{c_0}{2a}(\tfrac{3}{4}-l)\sin\phi\right\}\int_0^{\pi/2}\frac{\partial}{\partial\phi}\left\{\delta_0(y,t)\cos\psi\right\}\sin\psi\, d\psi \\ &= \frac{4SC_L'}{\pi C}\left\{1 + \frac{\delta_1}{\delta_0}\frac{c_0}{2a}(\tfrac{3}{4}-l)\sin\phi\right\}\int_0^{\pi/2}\frac{a^4\cos^2\psi}{8(a^4 - s^4\cos^2\phi\cos^2\psi)}\, d\psi \\ &= \frac{4SC_L'}{\pi C}\left\{1 + \frac{\delta_1}{\delta_0}\frac{c_0}{2a}(\tfrac{3}{4}-l)\sin\phi\right\}\frac{\pi a^4}{16s^4}\sec^2\phi\left\{\frac{a^2}{\sqrt{(a^4 - s^4\cos^2\phi)}} - 1\right\}.\end{aligned}$$

Therefore

$$\begin{aligned}\delta &= \frac{a^4}{\pi s^4}\int_0^{\pi/2}\left\{1 + \frac{\delta_1}{\delta_0}\frac{c_0}{2a}(\tfrac{3}{4}-l)\sin\phi\right\}\left\{\frac{a^2}{\sqrt{(a^4 - s^4\cos^2\phi)}} - 1\right\}\tan^2\phi\, d\phi \\ &= -\frac{a^4}{\pi s^4}\int_0^{\pi/2}\left\{\tan\phi + \frac{\delta_1}{\delta_0}\frac{c_0}{2a}(\tfrac{3}{4}-l)\sec\phi\right\}\frac{d}{d\phi}\left\{\sin^2\phi\left[\frac{a^2}{\sqrt{(a^4 - s^4\cos^2\phi)}} - 1\right]\right\} d\phi \\ &= \frac{1}{\pi k^2}\left[\left\{\frac{\pi}{2} - E_1\right\} + \frac{\delta_1}{\delta_0}\frac{c_0}{2a}(\tfrac{3}{4}-l)\left\{2 - \sqrt{(1-k^2)} - \frac{1}{k}\sin^{-1}k\right\}\right],\end{aligned}$$

where*

$$E_1 = \int_0^{\pi/2}\sqrt{(1 - k^2\cos^2\phi)}\, d\phi$$

and

$$k = s^2/a^2\,.$$

A chart in the form of Figs. 2 and 3 can be obtained by substituting

$$\left.\begin{aligned} l &= \tfrac{1}{4} \\ k &= 4\sigma^2 \\ c_0/2a &= 8\sigma/\pi A \end{aligned}\right\},$$

and by taking the appropriate ratio δ_1/δ_0 from Table 6.

Octagonal Tunnels.—The interference on a wing placed symmetrically in a tunnel of octagonal section is best calculated by a method due to Batchelor, which is presented in a general form in Ref. 8 (1943). The upwash induced by the triangular corner fillets is expressed as

* Tabulated values of the complete elliptic integral E_1 will be found in *Tables of the Complete and Incomplete Elliptic Integrals* by Legendre with an introduction by Karl Pearson. Cambridge University Press, 1934.

an increment to the larger contribution induced by the basic rectangular tunnel. The derived formula expresses δ_0 in terms of the mean upwash along the span of a uniformly loaded wing. The values of $\delta_0(y,t)$, defined in this report, are given further consideration in Ref. 9 (1947), which extends the theory of Ref. 8 to calculate the interference on a half-wing in an octagonal tunnel.

The chordwise variation of upwash is obtained approximately by adding to its value in the basic rectangular tunnel an amount proportional to the corresponding increment to $\delta_0(y,t)$:

i.e.,
$$\frac{[\delta_1(y,t)] \text{ octagonal}}{[\delta_1(y,t)] \text{ rectangular}} = \frac{[\delta_0(y,t)] \text{ octagonal}}{[\delta_0(y,t)] \text{ rectangular}}.$$

$\frac{hb + C}{2hb}$ may be used as a rough approximation to this ratio.

Should tables of $\delta_0(y,t)$ and $\delta_1(y,t)$ be required for wings placed above or below the centre plane of the tunnel, the quantities should first be computed for the basic rectangular tunnel and then corrected in the above ratio to account for the corner fillets.

(1340) Wt. 18/9296 K.8 5/56 Hw.

Publications of the Aeronautical Research Council

ANNUAL TECHNICAL REPORTS OF THE AERONAUTICAL RESEARCH COUNCIL (BOUND VOLUMES)

1938 Vol. I. Aerodynamics General, Performance, Airscrews. 50*s*. (51*s*. 2*d*.)
Vol. II. Stability and Control, Flutter, Structures, Seaplanes, Wind Tunnels, Materials. 30*s*. (31*s*. 2*d*.)

1939 Vol. I. Aerodynamics General, Performance, Airscrews, Engines. 50*s*. (51*s*. 2*d*.)
Vol. II. Stability and Control, Flutter and Vibration, Instruments, Structures, Seaplanes, etc. 63*s*. (64*s*. 2*d*.)

1940 Aero and Hydrodynamics, Aerofoils, Airscrews, Engines, Flutter, Icing, Stability and Control, Structures, and a miscellaneous section. 50*s*. (51*s*. 2*d*.)

1941 Aero and Hydrodynamics, Aerofoils, Airscrews, Engines, Flutter, Stability and Control, Structures. 63*s*. (64*s*. 2*d*.)

1942 Vol. I. Aero and Hydrodynamics, Aerofoils, Airscrews, Engines. 75*s*. (76*s*. 3*d*.)
Vol. II. Noise, Parachutes, Stability and Control, Structures, Vibration, Wind Tunnels. 47*s*. 6*d*. (48*s*. 8*d*.)

1943 Vol. I. Aerodynamics, Aerofoils, Airscrews. 80*s*. (81*s*. 4*d*.)
Vol. II. Engines, Flutter, Materials, Parachutes, Performance, Stability and Control, Structures. 90*s*. (91*s*. 6*d*.)

1944 Vol. I. Aero and Hydrodynamics, Aerofoils, Aircraft, Airscrews, Controls. 84*s*. (85*s*. 8*d*.)
Vol. II. Flutter and Vibration, Materials, Miscellaneous, Navigation, Parachutes, Performance, Plates and Panels, Stability, Structures, Test Equipment, Wind Tunnels. 84*s*. (85*s*. 8*d*.)

Annual Reports of the Aeronautical Research Council—

1933–34	1*s*. 6*d*. (1*s*. 8*d*.)	1937	2*s*. (2*s*. 2*d*.)
1934–35	1*s*. 6*d*. (1*s*. 8*d*.)	1938	1*s*. 6*d*. (1*s*. 8*d*.)
April 1, 1935 to Dec. 31, 1936	4*s*. (4*s*. 4*d*.)	1939–48	3*s*. (3*s*. 2*d*.)

Index to all Reports and Memoranda published in the Annual Technical Reports, and separately—

April, 1950 - - - - R. & M. No. 2600 2*s*. 6*d*. (2*s*. 7½*d*.)

Author Index to all Reports and Memoranda of the Aeronautical Research Council—

1909–January, 1954. R. & M. No. 2570 15*s*. (15*s*. 4*d*.)

Indexes to the Technical Reports of the Aeronautical Research Council—

December 1, 1936 — June 30, 1939	R. & M. No. 1850	1*s*. 3*d*. (1*s*. 4½*d*.)
July 1, 1939 — June 30, 1945	R. & M. No. 1950	1*s*. (1*s*. 1½*d*.)
July 1, 1945 — June 30, 1946	R. & M. No. 2050	1*s*. (1*s*. 1½*d*.)
July 1, 1946 — December 31, 1946	R. & M. No. 2150	1*s*. 3*d*. (1*s*. 4½*d*.)
January 1, 1947 — June 30, 1947	R. & M. No. 2250	1*s*. 3*d*. (1*s*. 4½*d*.)

Published Reports and Memoranda of the Aeronautical Research Council—

Between Nos. 2251–2349	R. & M. No. 2350	1*s*. 9*d*. (1*s*. 10½*d*.)
Between Nos. 2351–2449	R. & M. No. 2450	2*s*. (2*s*. 1½*d*.)
Between Nos. 2451–2549	R. & M. No. 2550	2*s*. 6*d*. (2*s*. 7½*d*.)
Between Nos. 2551–2649	R. & M. No. 2650	2*s*. 6*d*. (2*s*. 7½*d*.)

Prices in brackets include postage

HER MAJESTY'S STATIONERY OFFICE

York House, Kingsway, London W.C.2 ; 423 Oxford Street, London W.1 (Post Orders : P.O. Box 569, London S.E.1) ; 13a Castle Street, Edinburgh 2 ; 39 King Street, Manchester 2 ; 2 Edmund Street, Birmingham 3 : 109 St. Mary Street, Cardiff ; Tower Lane, Bristol, 1 ; 80 Chichester Street, Belfast. *or through any bookseller*

S.O. Code No. 23-2881